



## Scalemic natural products

Cite this: *Nat. Prod. Rep.*, 2023, 40, 1647

Sarah Mazzotta,<sup>a</sup> Vincenzo Rositano,<sup>ab</sup> Luca Senaldi,<sup>b</sup> Anna Bernardi,<sup>id a</sup> Pietro Allegrini<sup>b</sup> and Giovanni Appendino<sup>id \*c</sup>

Covering: up to the end of 2022

The area of scalemic natural products is often enigmatic from a mechanistic standpoint, since low optical purity is observed in compounds having multiple contiguous stereogenic centers resulting from mechanistically distinct biogenetic steps. A scalemic state is rarely the result of a sloppy enzymatic activity, rather resulting from the expression of antipodal enzymes/directing proteins or from the erosion of optical purity by enzymatic or spontaneous reactions. Evidence for these processes is critically reviewed, identifying the mechanisms most often associated to the enzymatic generation of scalemic natural products and also discussing analytical exploitations of natural products' scalemicity.

Received 21st March 2023

DOI: 10.1039/d3np00014a

rsc.li/npr

1	<b>Introduction</b>
2	<b>Self-disproportionation of enantiomers (SDE) during the purification of scalemates</b>
3	<b>The origin of scalemic natural products</b>
3.1	<b>Partial racemization of enantiopure compounds</b>
3.1.1	<b>By enolization and tautomerization</b>
3.1.2	<b>By pericyclic process</b>
3.1.3	<b>By enzymatic activity</b>
3.2	<b>Co-expression of antipodal enzymes or directing proteins</b>
3.2.1	<b>Polyene cyclization</b>
3.2.2	<b>Iminium ion trapping</b>
3.2.3	<b>Radical coupling</b>
3.2.3.1	<b>Alkyl coupling</b>
3.2.3.2	<b>Aryl coupling</b>
3.2.4	<b>Oxidative modification of isoprenoid residues</b>
3.2.5	<b>Functionalization of non-isoprenyl unactivated carbons</b>
3.2.6	<b>Cycloaddition reactions</b>
4	<b>Strategies to upgrade the optical purity of scalemic natural products</b>
5	<b>Analytical applications of scalemic natural products</b>
6	<b>The importance of being scalemic: when optical impurity is advantageous</b>
7	<b>Conclusions</b>
8	<b>Author contributions</b>
9	<b>Conflicts of interest</b>

10	<b>Acknowledgements</b>
11	<b>Notes and references</b>

## 1 Introduction

The occurrence of different enantiomeric forms of natural products can be traced back to the early 19th century observation of an opposite optical rotation in French and American turpentine, with French turpentine being laevorotatory and American turpentine dextrorotatory.<sup>1</sup> Turpentine was one of the first organic substances discovered to show optical activity, and enantiomeric forms of  $\alpha$ -pinene (**1**, Fig. 1) occur indeed in its source plants (*Pinus maritima* L. for French turpentine and mainly *P. palustris* Mill for American turpentine).<sup>1</sup> The existence of racemic natural products, that is of an equimolar mixture of both enantiomers in a single producer, was actually first reported with compounds better referred to as *racemized* rather than *racemic*, since loss of enantiomeric purity had occurred during extraction and/or isolation, as in paratartaric (racemic) acid (( $\pm$ )-2)<sup>2</sup> and atropine (( $\pm$ )-3),<sup>3</sup> but truly racemic natural products were then shown to exist, and certain biogenetic pathways are now recognized to be significantly associated to the generation of racemic natural products.<sup>4</sup> More puzzling is the occurrence of scalemic (enantiomerically enriched) natural products, not only simple monoterpenes like  $\alpha$ -pinene (**1**), known to occur as (+)-, (-)-, ( $\pm$ )- $\alpha$ -pinene as well as in various ratios of its enantiomers,<sup>5</sup> but also more complex and polycyclic compounds like the meroterpene *cis*- $\Delta^9$ -tetrahydrocannabinol (**4**)<sup>6</sup> and the alkaloid cephalotaxine (**5**).<sup>7</sup> The number of these occurrences increased with the advent of chiral HPLC as routine analytical tool for natural product mixture. The occurrence of natural scalemates is apparently ambiguous, since chiral

<sup>a</sup>Dipartimento di Chimica, Università degli Studi di Milano, Via Golgi 19, 20133 Milano, Italy

<sup>b</sup>Indena SpA, Via Don Minzoni 6, 20049 Settala, MI, Italy

<sup>c</sup>Dipartimento di Scienze del Farmaco, Largo Donegani 2, 28100 Novara, Italy. E-mail: giovanni.appendino@uniupo.it



natural products are either made by enzymes, and are therefore expected to be enantiomerically pure, or spontaneously self-assemble from reactive species generated by enzymes, and are therefore expected to be racemic [or a mixture of diastereomers in case of pre-existing stereogenic element(s)].<sup>4</sup> Scalemates are a bump in the road, a deviance from a binary logic (enantiomeric purity or racemic state) also plagued by semantic problems. Thus, *racemic* refers to an equimolar mixture of two enantiomers, and has therefore an associated numeric value, while *scalemic* refers to an uneven ratio of two enantiomers, and is only qualitative, covering a whole spectrum of values. Methodologic limits also exist, and absolute enantiomeric purity and absolute lack of enantiomeric purity are pure abstractions, the ends of a continuous line, with the meaning of “high enantiomeric purity” being context-dependent. In the analysis of terpene hydrocarbons, a class of compounds generally highly scalemic or even racemic, a 90 : 10 enantiomeric ratio could be reported as a noteworthy enantiomeric purity, while in a pharmaceutical context a ratio lower than 99 : 1 could cause concern and require additional purification. A similar situation exists in

the literature on enantioselective synthesis, where the bar of enantiomeric purity has been constantly raised. The first enantioselective reaction was reported by Bredig and Fiske in 1912,<sup>8</sup> and produced, under quinine catalysis, mandelonitrile (**6**) from two achiral precursors (benzaldehyde and hydrocyanic acid) in *ca* 8% enantiomeric excess (ee). Conversely, the first disclosure of the sharpless asymmetric dihydroxylation in 1988 reported crude ee >95% for *trans*-stilbene as a substrate,<sup>9</sup> and ee > 99% are nowadays not uncommon in the literature on asymmetric synthesis.

A notation problem also exists. While enantiomerically pure compounds can be drawn according to their absolute configuration (when known) and racemates can be indicated by ( $\pm$ ) or “*rac*”, there is not accepted notation for scalemates. In this review, for compounds with a single stereogenic element (center or axis) we do not draw configurations for scalemic forms. For compounds with multiple stereocenters, we draw the configuration of the predominant isomer. Information about its enantiomeric composition must be found in the text.



*Sarah Mazzotta received her Master's degree from the University of Calabria in 2016 and she obtained her PhD at University of Seville (2020). Her PhD research activity was focused on the design and synthesis of novel antimicrobial small molecules, especially against adenovirus infections. She was also involved in the preparation of new bioactive compounds from natural sources.*

*Since 2020, she is a postdoctoral research fellow at the University of Milan and she works on the generation of novel glycomimetics as bacterial lectin ligands useful in anti-adhesion therapy for microbial diseases.*



*Vincenzo Rositano received his Bachelor's (2017) and Master's degree (2019) from the University of Pisa under the supervision of Prof. Anna Iuliano, working on asymmetric catalysis. In 2021 he moved to Milan where is now pursuing his doctoral study at University of Milan, in partnership with Indena. His research is focused on the development of processes for industrial preparation of*

*active pharmaceutical ingredients, from plant and microbial origin.*



*Luca Senaldi received his Bachelor's (2014) and Master's degree (2016) from the University of Milan under the supervision of Prof. Anna Bernardi. In 2020 he received his PhD degree from the University of Milan at the end of the high-level apprenticeship period at Indena, a company specialized in the preparation of pharmaceutical and food ingredients. He is currently working at*

*Indena Research and Development and his research focuses on the design and development of processes for the industrial preparation of active pharmaceutical ingredients.*



*Anna Bernardi obtained her PhD at the Università degli Studi di Milano in 1986. After a post-doctoral period at Columbia University (NY), she returned to Milano in 1989 as a research associate and became full professor of Organic Chemistry in 2005. She has worked on the development of stereoselective methodologies in organic synthesis, the design of new reagents and, for the past 20*

*years, on the design and synthesis of carbohydrate mimics (glycomimetics). She received the Quilico Medal of the Società Chimica Italiana in 2021.*



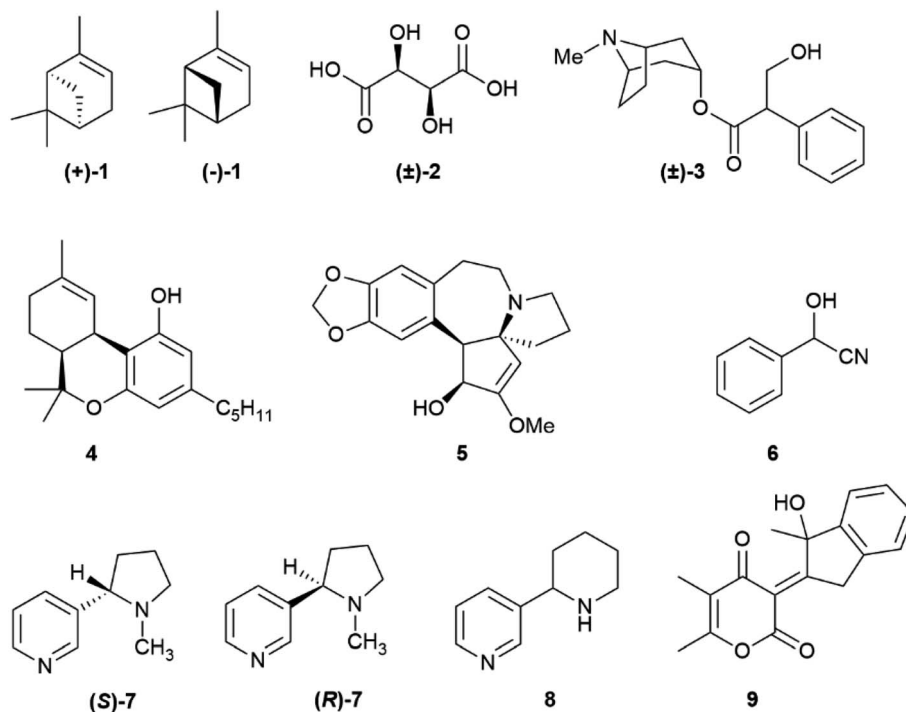


Fig. 1 Chemical structures of compounds 1–9.

The occurrence of racemic natural products has been the subject of several recent reviews,<sup>10–15</sup> one comprehensively covering the years 2012–2019.<sup>15</sup> Conversely, the grey area of natural products' optical "impurity" (scalemicity) has so far been largely overlooked, and the inventory of scalemic natural products is probably underestimated for various reasons. The first one is that the optical purity of novel natural products is rarely reported, and novel natural products are assumed, when chiral and optically active, to be also enantiomerically pure. Thus, out of the 286 articles reporting novel chiral natural products published by the *Journal of Natural Products* in 2017,

enantiomeric purity was evaluated only in 31 articles (<15%).<sup>16</sup> The second reason is that, as discussed in the next section, whenever a highly scalemic mixture is subjected to a physico-chemical process that involves a phase change (evaporation, crystallization, achiral chromatography), self-disproportionation of enantiomers (SDE) can occur, with a redistribution between the two phases. As a result, for highly scalemic compounds, optical purity is generally upgraded in the mother liquors of crystallization and in the faster moving chromatographic fractions, and downgraded in the complementary phase or fractions.<sup>17</sup> Since the physical and



Pietro Allegrini received his BS/MS degree from the University of Milan in 1987 and completed the specialization course in Chemical Synthesis at the University of Milan in 1991. He is currently the Research and Development Director at Indena SpA. His research activity has been devoted to process chemistry applied to the industrial synthesis of fine chemicals and active pharmaceutical ingredients as well as natural products. He is co-founder of ISPROCHEM, an international school of process chemistry. In 2018 he has been awarded with the Industrial Research Prize of the Italian Chemical Society – Organic Chemistry division.

He is co-founder of ISPROCHEM, an international school of process chemistry. In 2018 he has been awarded with the Industrial Research Prize of the Italian Chemical Society – Organic Chemistry division.



Giovanni Appendino is Emeritus Professor at the University del Piemonte Orientale, Department of Pharmaceutical Sciences, Novara (Italy). His research activity has focused on the isolation, chemical modification, and total synthesis of bioactive natural products of plant origin. His studies were recognized by the Italian Chemical Society (Quilico- and Piria medals), by the Phytochemical Society of Europe (Rhône-Poulenc Rorer award and Bruker prize) and by GA (Honorary membership).

His studies were recognized by the Italian Chemical Society (Quilico- and Piria medals), by the Phytochemical Society of Europe (Rhône-Poulenc Rorer award and Bruker prize) and by GA (Honorary membership).



spectroscopic properties of novel natural products are preferentially reported on compounds carefully purified by chromatography and/or crystallization, the possibility exists that scalemates could potentially be reported as racemates or quasi-racemates. Finally, a compound can be produced as a scalemate and then upgraded to enantiomeric purity by enzymatic activity, nicotine being a remarkable example. Nicotine is produced in the roots of the tobacco plant (*Nicotiana tabacum* L.) as a scalemate, with (*S*)-nicotine ((*S*)-7) as the dominant enantiomer by a factor of *ca* 95 : 5. However, during xylemic translocation to the leaves, (*R*)-nicotine ((*R*)-7) is enantioselectively *N*-demethylated, resulting in high optical purity (>99%) for the alkaloid isolated from the leaves.<sup>18</sup> Interestingly, anabasine (**8**), the teratogenic piperidine homologue of nicotine, is not significantly accumulated in tobacco leaves, and only occurs, in a highly scalemic form, in the stalks,<sup>19</sup> an observation highlighting the relevance of the *N*-methyl group, present in nicotine but not in anabasine, as a “handle” for the enzymatic “resolution” of nicotinoid alkaloids. Incidentally, (*R*)-nicotine is significantly more toxic than (*S*)-nicotine, but has a lower affinity for cholinergic receptors and almost negligible recreational activity. The presence of synthetic racemic nicotine in “tobacco-free” e-cigarettes liquids is therefore potentially dangerous, since consumers, by dosing their puffs with (*S*)-nicotine ((*S*)-7), also inhale significant amounts of the more toxic (*R*)-enantiomer ((*R*)-7).<sup>20</sup>

The purpose of this review is to foster attention on scalemate natural products, highlighting that the optical purity of novel compounds cannot be taken for granted, especially for some classes of natural products, and should be validated by chiral analysis, either spectroscopic or chromatographic. We do not aim to provide a comprehensive list of natural scalemates, inevitably incomplete for the reasons discussed above, but rather to identify biogenetic pathways and mechanisms associated to the generation of scalemate natural products, highlighting the areas most in need of investigation and discussing the opportunity that scalemic natural products offer to biomedical research.

## 2 Self-disproportionation of enantiomers (SDE) during the purification of scalemates

Any type of physicochemical operation which involves phase separation (crystallization, solubilization, chromatography, distillation, sublimation) has the potential to alter the composition of scalemates, differently redistributing them into enantio-enriched and enantio-depleted phases.<sup>17,20</sup> For compounds with significant volatility, even trivial operations like solvent removal by rotary evaporation<sup>21,22</sup> or vacuum drying<sup>23</sup> have been reported to produce scalemates enantioenriched by the loss of the faster evaporating/sublimating racemate. In asymmetric synthesis, it is generally possible to avoid fractionation and directly measure ee on crude reaction mixtures by chiral chromatography or by NMR. Conversely, the complexity of biomass extracts makes extensive

chromatographic steps, often associated to crystallization, mandatory to reach a purity level sufficient for the structure elucidation and the determination of enantiomeric purity of isolated natural products. Thus, SDE is unavoidable, at least to some degree, and especially in compounds highly functionalized and prone to intermolecular interactions.<sup>17,24</sup> For this reason, it is difficult to go beyond the identification of the dominant enantiomer and to make a quantitative comparison between the ee of natural scalemates from different sources and/or different purification processes.

SDE has so far received scarce attention within the natural products community, even though the first systematic studies in the area can be traced back to a series of seminal observations by Otto Wallach on crystal terpene derivatives.<sup>25</sup> Working with brominated carvones, Wallach reported in 1895 that racemic crystals tend to be denser and have a higher melting point and a lower solubility than their homochiral analogues (Wallach rule).<sup>26</sup> Although exceptions are known, racemic crystals, representing more than 90% of the crystalline racemic mixtures, are generally more tightly packed and thermodynamically more stable than their enantiopure counterparts.<sup>26</sup> A chiral packing can be accommodated only in a limited set of the crystallographic space groups, which are, conversely, all available for racemic crystals. Crystallization of a scalemate can therefore afford racemic or quasi-racemic crystals even from highly biased scalemic mixtures.<sup>26</sup> A remarkable example was reported by Sharpless in *Organic Synthesis*, describing the upgrade of the ee of a diol obtained by asymmetric dihydroxylation from 84% to 97% by selective crystallization of a quasi-racemate of the minor enantiomer.<sup>27</sup> Mixtures of racemic and enantiopure crystals can, in principle, be separated based on their different density, and ultracentrifugation has indeed been reported to efficiently separate mechanical mixtures of racemic and enantiopure crystals of alanine.<sup>28</sup> The situation is well summarized by ternary diagrams of solubility phase (Fig. 2).<sup>29</sup> The racemate is characterized by two eutectic points (E and E') that define five different regions. The upper region (A-1) corresponds to the non-saturated solution, and the two lateral triangles (A-2) to pure crystals of each enantiomers. Adjacent to the A-2 phases, two triangular regions (A-3) represent

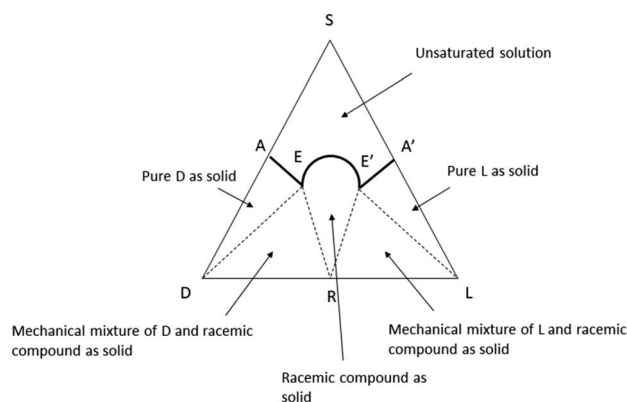


Fig. 2 Ternary solubility diagram of true racemic compounds.



mechanical mixtures of racemate and enantiopure crystals, while the central conical phase corresponds to the racemate (A-4). A scalemate whose composition falls in the E-E' projection at the base of the triangle will produce a racemate, while scalemates whose composition correspond to the AE and A'E projections will afford pure enantiomers. A decrease of temperature and the presence of groups that favour intermolecular interactions will raise the vertex of the solubility curve, enlarging the E-E' projection, and favouring the crystallization of a racemate. The phase diagram clearly shows that if the composition of the scalemic mixture has high content of one of the enantiomers, it is probable to end in the pure D and pure L solids regions and hence the enantiomeric composition can be further enriched. On the other hand, when the starting composition of the mixtures is close to racemic ratios (R), the obtained crystals are often racemic. Anyway, in both the cases the starting scalemic mixture is altered by crystallization.

“Optical purification” by crystallization makes it possible that natural products reported as crystalline racemates could actually be scalemates, with loss of optical rotation being associated not to the removal of impurities, but to self-disproportionation. This was shown for the fungal ketide colletopyrandione (9, Fig. 1), which occurs as a scalemate in extracts but crystallizes as a racemate,<sup>30</sup> and SDE tests should be applied to assess its contribution to the isolation of a crystalline racemate natural product. In this context, it should be remarked that the measurement of optical purity is sensitive to the presence of impurities, especially when a compound has low optical rotation, and the same holds for electronic circular dichroism (ECD) when the impurity has UV absorption similar to the one of the main product. When the presence of a scalemate is suspected, it is therefore advisable to rely on a chromatographic determination of enantiomeric composition or on NMR derivatization with chiral reagents, rather than simply on measurement of optical rotation.

The considerations discussed for crystallization hold also for other preparative processes of purification, like

chromatography, distillation, and sublimation. The last technique is not of general relevance for natural products purification, but chromatography is also the largest area of SDE manifestation, since applicable to all scalemates independently on their physical state. Dreiding was one of the first to warn that achiral chromatography should be used with great care for the purification of scalemates, since the enantiomeric composition of chromatographically pure fractions is affected by the different solubility of racemic and enantiopure crystals in the eluent.<sup>31</sup> Similar observations were also reported by Kagan,<sup>32</sup> but, despite the gigantic state of Dreiding and Kagan in stereochemical studies, the research community has so far largely failed to receipt these warning notes. The issue of scalemate chromatography is particularly challenging for natural products, since crude extracts contain a host of optically pure small molecules, whose solubilization renders *de facto* non-achiral the chromatographic eluant. For these reasons, it is not unconvivable that the racemic state of some natural products might be dubious and in need of re-evaluation, while early measurements of ee, especially with chiral NMR or chiral chromatography, should be used to investigate differences in the stereochemical state of native and isolated natural products.

## 3 The origin of scalemic natural products

### 3.1 Partial racemization of enantiopure compounds

Partial racemization during isolation and/or purification is the most obvious reason for the isolation of a natural product in a scalemic form, but post-synthetic erosion as well as upgrade of optical purity are also documented. Two major types of mechanisms underlie the spontaneous erosion of optical purity, namely enolization and pericyclic reactivity.

**3.1.1 By enolization and tautomerization.** The best known example of deprotonation-induced erosion of optical purity is atropine ((±)-3, Fig. 3). This tropane alkaloid occurs in plant as optically pure (S)-(-)-L-hyoscyamine ((S)-3), but due to the acidity

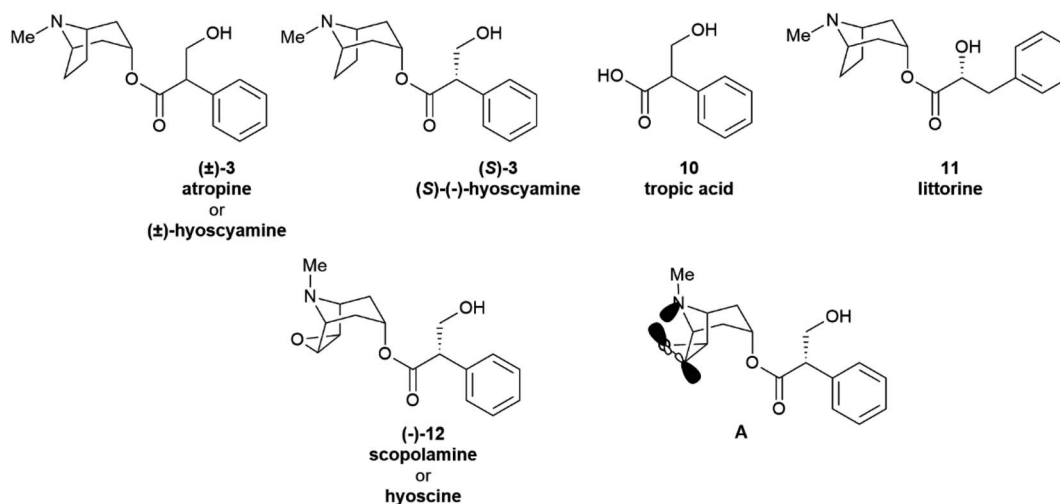


Fig. 3 Tropane alkaloids and related compounds.



of the benzylic  $\alpha$ -proton of tropic acid (**10**) and the inherent basicity of the tertiary amine group ( $pK_a = 9.85$ ), (–)-hyoscyamine self-racemizes at room temperature, especially in protic solvent, turning into atropine [(±)-hyoscyamine, (±)-**3**].<sup>33</sup>

The stereogenic center of tropic acid is established at the level of the phenyllactate ester of tropine (littorine, **11**, Fig. 3) *via* a process mediated by an oxidative rearrangement induced by an iron-based oxygenase (CYP80F1). After initial homolyses of the benzylic C–H bond from the high-valent oxo-iron species (Scheme 1), rearrangement of the carbon-centered benzyl radical to the oxygen-centered cyclopropanol radical **13** occurs, with hydroxyl radical rebound eventually taking place at the homobenzyl carbon and not at the one where the original radical was generated (Scheme 1).<sup>34</sup> This process is strictly stereoregulated, and the side-chain stereogenic center of the tropic acid moiety of **11** is generated with high selectivity for the *S* configuration. The two enantiomers of hyoscyamine have distinct biological profiles. Thus, most cholinergic activity resides in the natural *S*-(–)-enantiomer, but (+)-hyoscyamine has, surprisingly, more potent excitatory effects on the central nervous system.<sup>35</sup> Because of this, and to secure standardization of dosages, the European Pharmacopoeia requires that the optical purity of atropine (**3**), expressed as (–)-hyoscyamine ((–)-**3**), should not exceed 9%.<sup>36</sup>

Remarkably, the self-catalysed racemization of the closely related alkaloid scopolamine (hyoscyne, (–)-**12**, Fig. 3) to atropine ((±)-**12**) is slower than the one of hyoscyamine to atropine, since, despite the structural similarity between the two alkaloids, scopolamine is significantly less basic than hyoscyamine ( $pK_a$  7.60 *vs.* 9.85).<sup>37</sup> This difference is presumably due to a combination of the inductive effects associated to the oxirane oxygen as well as to homoanomeric donation of the nitrogen lone pair on the  $\sigma_{C-O}^*$  bonds of the epoxide ring (**A**, Fig. 3). In contrast to hyoscyamine, where it occupies a pseudo-axial orientation, in scopolamine the nitrogen lone-pair is pseudo-equatorially orientated, which allows orbital interaction with the carbon–oxygen bonds of the oxirane.<sup>38</sup> Despite the structural similarity of atropine (**3**) and scopolamine ((–)-**12**) the European Pharmacopoeia requires tests of optical “impurity” for the former and of optical “purity” for the latter ( $[\alpha]_D -33$  and  $-39$ ).<sup>36</sup>

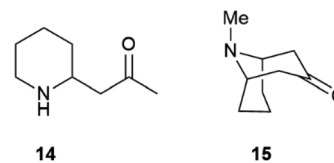
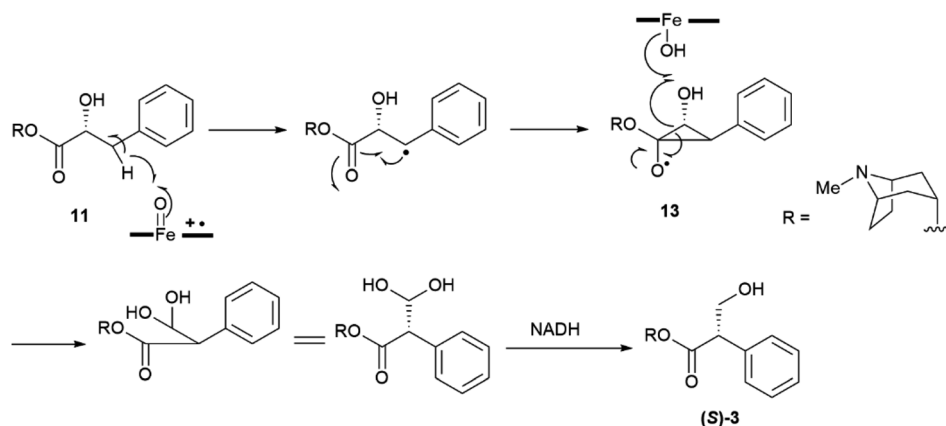


Fig. 4 Pelletierine **14** and pseudopelletierine **15**.

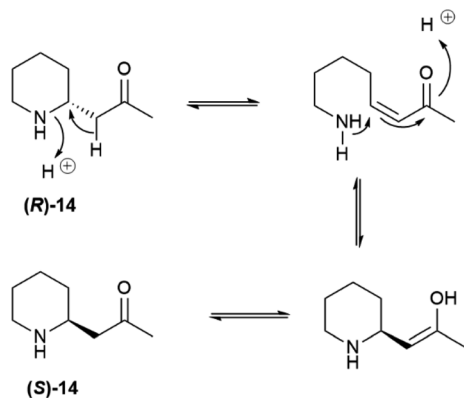
Partial self-racemization also underlies the long controversies on the structure of pelletierine (**14**), the major alkaloid from pomegranate root bark (Fig. 4). This piperidine alkaloid was first isolated in 1878 by Tanret in France, and named after Joseph Pelletier (1788–1842), one of the founding fathers of alkaloid research.<sup>39</sup> After salification, pelletierine (**14**) could be crystallized both in an optically active laevorotatory form and a racemate. The latter was assumed by Tanret to be an isomer of the laevorotatory compound and named isopelletierine, while a related, optically inactive, alkaloid was referred to as pseudopelletierine (**15**).<sup>39</sup> Pseudopelletierine (**15**), an achiral compound, holds a special position in the history of chemistry, since it was the starting material for Wilstaetter's synthesis of cyclooctatetraene, a compound that fostered interest in the nature of aromaticity.<sup>40</sup>

Pelletierine and isopelletierine were considered constitutional isomers, the former being an aldehyde and the latter a ketone. In a further bold development to reconcile the failure to correlate isopelletierine to the hemlock alkaloid conidrine (see *infra*), pelletierine and isopelletierine were considered no longer constitutional isomers but diastereomers, assuming the presence of a stereogenic non-inverting nitrogen in both compounds.<sup>41</sup> The structure of isopelletierine was eventually unambiguously solved by Meissenheimer, who synthesized it from 2-methylpyridine, while the discovery that pelletierine is configurationally labile in the presence of bases finally clarified its relationship with isopelletierine.<sup>41</sup> The configurational lability of pelletierine is due to retro-aza-Michael equilibration with an open form (Scheme 2), a process base-catalyzed and almost unavoidable in the standard workflow of alkaloid isolation, which involves extraction



Scheme 1 Oxidative rearrangement of the hydroxyphenyllactic acid ester **11** to (–)-hyoscyamine ((*S*)-**3**) *via* the cyclopropanol **13**.





Scheme 2 Racemization of pelletierine (**14**) via retro-aza-Michael fragmentation.

with acids of the plant material and then basification of the extract to recover its basic constituents.<sup>41</sup> In contrast, crystalline salts of pelletierine are remarkably stable toward racemization, and an analysis of the original Tanret sample of pelletierine sulfate carried out 80 years after its preparation showed substantial retention of optical purity.<sup>42</sup>

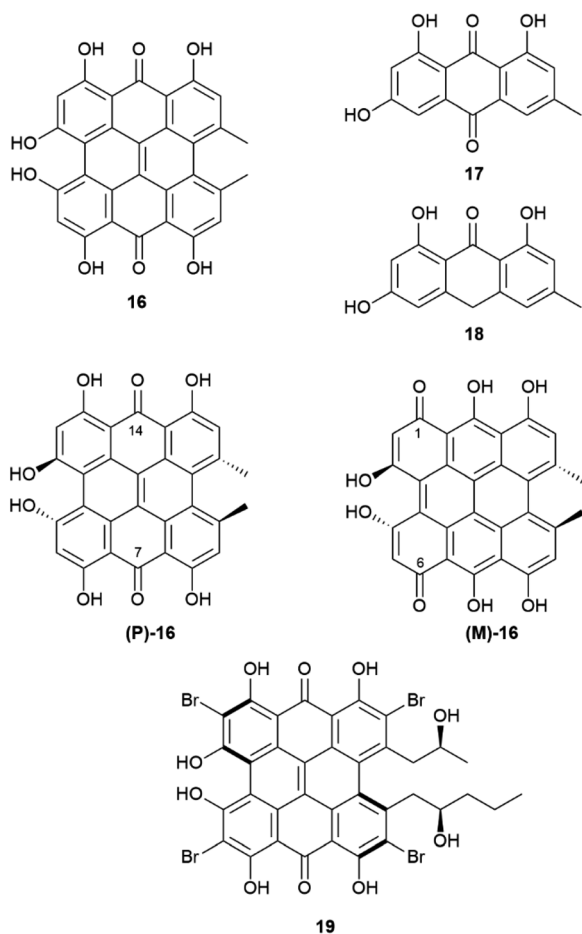
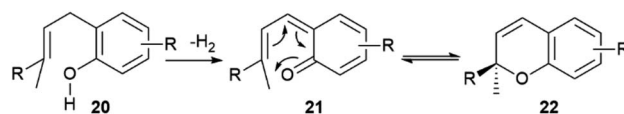


Fig. 5 Hypericine **16**, its biosynthetic precursors **17** and **18** and its two chiral tautomers (P)-**16** and (M)-**16**. Structure of the hypericin-related pigment gymnochrome A (**19**).

In conclusion, the major pomegranate alkaloid is synthesized in the plant in optically active form as pelletierine ((*R*)-**14**), which then partially isomerizes to isopelletierine ((*S*)-(+)-**14**). To avoid confusion, the name pelletierine should be used for the optically active native compound, and *rac*-pelletierine ((±)-**14**) for its racemized version. In sharp contrast with nicotine-related alkaloids, tropane and tropane-related alkaloids are therefore produced in an enantioselective way, and their isolation as scalemates or racemates is due to spontaneous racemization induced by the presence of an easily enolized carbonyl.

A complex set of tautomeric and rotameric equilibria is also responsible for enantiopurity erosion of the phenanthroperylenequinone hypericin (**16**, Fig. 5).<sup>43</sup> This phototoxic red pigment has been isolated from plants, insects and protozoa, but its best known source is St. John's worth (*Hypericum perforatum* L.), in whose flowering toppings it can occur in concentrations as high as 0.3% on dry weight basis.<sup>44</sup> Hypericin is responsible for hypericism, a potentially deadly sun-dependent intoxication of farm animals. It has been suggested that hypericin derives from emodin (**17**) or emodin anthrone (**18**) by oxidative dimerization associated to a single phenol oxidase coupling protein (Hyp-1).<sup>44</sup> Hypericin shows a remarkable structural complexity, not evident from a superficial inspection of its formula, and associated to torsional and tautomeric equilibria.<sup>45</sup>

In short, two sets of axially chiral tautomers exist ((*P*)-**16** and (*M*)-**16**), differing for the location of the quinone moiety on the central (7,14-tautomer (*P*)-**16**) or on the peripheral (1,6-tautomer (*M*)-**16**) biphenyl systems. In the solid state, the least stable 1,6-peripheral quinone system ((*M*)-**16**) prevails in salts, while the more stable 7,14-tautomer ((*P*)-**16**) prevails in the non-ionized compounds.<sup>46,47</sup> All tautomers have a propeller  $C_2$ -symmetric and chiral shape, and racemization occurs *via* interconversion of *P* (*aS*) and *M* (*aR*)-tautomers. The racemization barrier is low, *ca* 20 kcal mole<sup>-1</sup>, with a half-life of around 30 minutes at 35 °C. Therefore, hypericin is obtained by isolation under normal room temperature conditions as a racemic compound.<sup>45</sup> On the other hand, in cell environment, hypericin could be present in an enantiopure *P*-configuration, stabilized by chiral interaction with other chiral molecules, and evidence has been obtained by investigating the association of hypericin with albumin.<sup>46</sup> This enantiomer has, indeed, a CAS number (548-04-9), and is, apparently, commercialized, although the synthetic origin of this material implies confusion with *rac*-hypericin, having CAS number 1372719-41-9. In principle, by working at low temperature (4 °C), it could be possible to isolate or resolve hypericin, since its enantiomers show a reasonable configurational stability at 15 °C. On the other hand, substituted hypericins like



Scheme 3 Generation of the chromene system **22** by tandem dehydrogenation-electrocyclization of *o*-isoprenylphenols (R = prenyl, geranyl).



the marine pigment gymnochrome A (**18**) and related compounds, were isolated in optically active form. Regrettably, optical purity was not reported.<sup>46</sup>

**3.1.2 By pericyclic process.** The 2,2-disubstituted chromene moiety (**22**) occurs in natural products from both terrestrial and marine organisms, and its formation is triggered by the FAD-dependent dehydrogenation<sup>48</sup> of an *o*-isoprenylphenolic (**20**) to a reactive vinylogous quinonmethide (**21**) which next undergoes thermal electrocyclicization to a 2,2-substituted chromene (Scheme 3).<sup>48,49</sup>

When the isoprenyl group is higher than a prenyl (geranyl, farnesyl), a stereogenic carbon is generated in the pericyclic process, and the resulting chromenes are chiral. Since the electrocyclicization is rapid and the intermediate vinylogous quinonmethides are generated in the chiral environment of the dehydrogenase enzyme,<sup>48</sup> the stereogenic carbon is seemingly generated in an enantiopure form, and many chromenes are, indeed, isolated in high enantiomeric purity (e.g. daurichromenic acid (**23**) from, various *Rhododendron* species).<sup>50</sup> However, cycloreversion during biomass storage followed by spontaneous electrocyclicization can erode this purity, with formation of highly scalemic or almost racemic compounds, as exemplified by cannabichromene (CBC, **24a**) from *Cannabis sativa* L. and by rhodonoids, a class of compounds derived from its tetra-nor analogue **24b** and occurring in *Rhododendron* species.<sup>51–53</sup>

Cycloreversion is induced by light and, to a lesser extent by heating, and is not significantly affected by treatment with acids and bases.<sup>53</sup> Reversibility of the electrocyclicization critically depends on the substitution pattern of the aromatic ring. The presence of a carboxylic group *para* to the chromenic oxygen significantly slows cycloreversion, an effect presumably due to stabilization by resonance of the aromatic ground-state, which leads to an increased activation energy for dearomatization (Scheme 3, conversion of **22** to **21**).<sup>48</sup> Cannabichromene (CBC, **24a**) and its analogues with a modified alkyl group<sup>54</sup> are the starting material for the generation of other phytocannabinoids, which are therefore expected to be scalemic. However, cannabicyclol (**25**), obtained from cannabichromene (CBC, **24a**) by photochemical or acidic cyclization,<sup>49</sup> was always isolated as a racemic compound, even though the stereogenic carbon of the starting chromene (**24a**) is not involved in the process (Fig. 6).

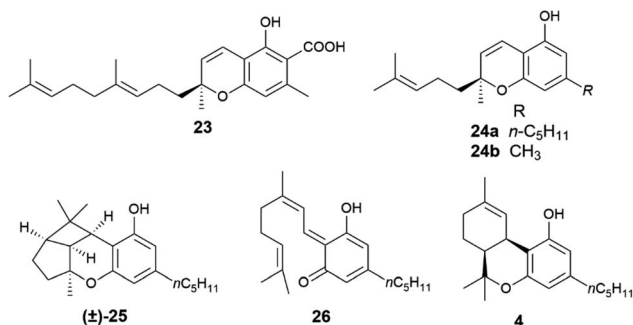


Fig. 6 Formulae of compounds 23–26 and 4.

Unlike its *trans*-isomer, a highly enantiopure compound,<sup>51</sup> *cis*- $\Delta^9$ -tetrahydrocannabinol (*cis*- $\Delta^9$ -THC, **4**) is scalemic,<sup>6</sup> and could derive from an intramolecular hetero-Diels–Alder cycloaddition of the vinylogous quinonmethide **26** where the  $\omega$ -, and not the proximal, trisubstituted double bond is involved in the pericyclic process (Scheme 3, R = prenyl).

**3.1.3 By enzymatic activity.** The “unnatural” *D*-versions of various proteinogenic amino acids occur in secondary metabolites from both microorganisms and metazoans, and is the result of a specific racemase activity<sup>55,56</sup> not associated, with the exception of some leguminous plants, to the accumulation of free *D*-amino acids (Fig. 7). The *D*-version of the proteogenic amino acids is generally metabolically active, serving as a building block for complex architectures or as a regulatory agent. *D*-(*R*)-serine (**27**) and *D*-(*R*)-glutamic acid (**28**) are essential constituents of the bacterial cell wall peptidoglycan, and therefore these amino acids occur in bacterial hydrolyzates as scalemates.<sup>55</sup>

*D*-amino acids play a relevant role also in mammalian metabolism, resulting into an overall scalemic state in some organs and at specific development stages. Thus, significant amounts of *D*-serine (**27**) occur in rat brain from birth until seven months of age.<sup>57</sup> The production of this amino acid then decreases and remains associated to the function of glutamate receptors of the *N*-methyl-*D*-aspartate (NMDA) type, where *D*-serine behaves as an endogenous agonist, acting at the strychnine-insensitive glycine site.<sup>57</sup> While *D*-serine only occurs in brain, *D*-aspartic acid (**29**) also occurs in other organs, undergoing development-dependent changes with age.<sup>58</sup> In the prefrontal cortex of human brain, aspartic acid was found to be scalemic, with dominance of the *D*-enantiomer by a 6 : 4 ratio at week 14 of gestation, and a decrease to trace level by week 41.<sup>59</sup> Just like *D*-serine (**27**), also *D*-aspartic acid binds to NMDA receptors at the strychnine-insensitive glycine site.<sup>58</sup> *S*-[L, (+)]. Lactic acid ((*S*)-**30**) is produced enantioselectively in glycolysis, but bacteria can invert its configuration, resulting in a generally scalemic or even racemic state for lactic acid of microbial origin.<sup>60</sup> The formation of (*R*)-*D*-lactic acid ((*R*)-**30**) is involved in the mechanism of bacterial resistance to vancomycin.<sup>60</sup> This glycopeptide antibiotic inhibits peptidoglycan synthesis by complexing the terminal *D*-Ala-*D*-Ala sequence of the peptidoglycan precursor. Replacement of the terminal *D*-alanine with *D*-lactic acid confers resistance to vancomycin, as does the replacement with *D*-serine (**27**).<sup>60</sup>

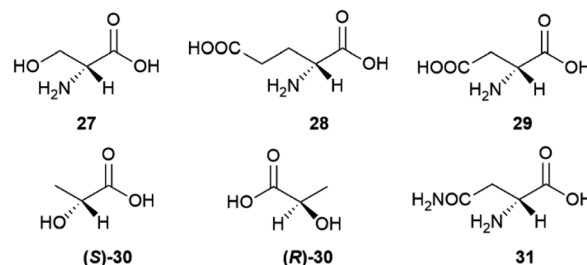
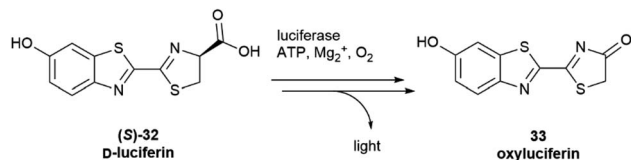


Fig. 7 Structures of the proteinogenic amino acids 27–29 and the hydroxyacids 30–31.







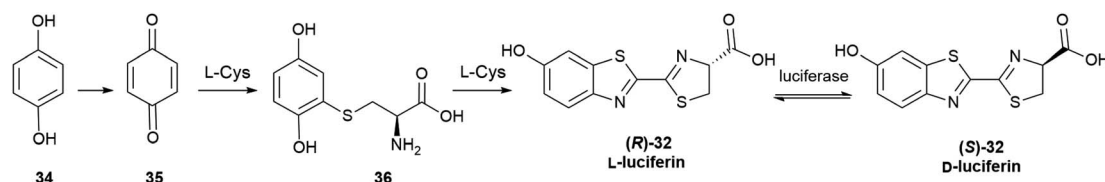
Scheme 4 The oxidation of D-luciferin (S)-32 by luciferase is the basis of luciferin bioluminescence.

For unclear reasons, some plants produce and accumulate significant amounts of D-amino acids in free form along with their proteinogenic version.<sup>55</sup> A remarkable case is represented by asparagine, which is accumulated as a scalemate in the initial phases of seed germination by various leguminous plants. The non-proteinogenic D-enantiomer (31) is then metabolized, eventually resulting in the selective accumulation of the natural L-form in adult tissues.<sup>61</sup> The scalemate state of asparagine in leguminous seeds was discovered by Arnaldo Piutti in 1886 in vetches (*Vicia sativa* L.) seedlings, and his observation of the distinct taste of the two enantiomers of this amino acid was the first report of different physiological effects associated to a pair of enantiomers.<sup>61,62</sup> In the wake of the studies by Guareschi on asparagine,<sup>63</sup> Piutti crystallized 20 kg of the L-enantiomer from an aqueous extract of 6.5 metric tons of germinated vetches, obtaining then a second crop of crystals from the mother liquors. Much to his surprise, the second crystal crop was a conglomerate of hemihedral crystals, from which, by manual (!) separation, he eventually obtained 100 g of

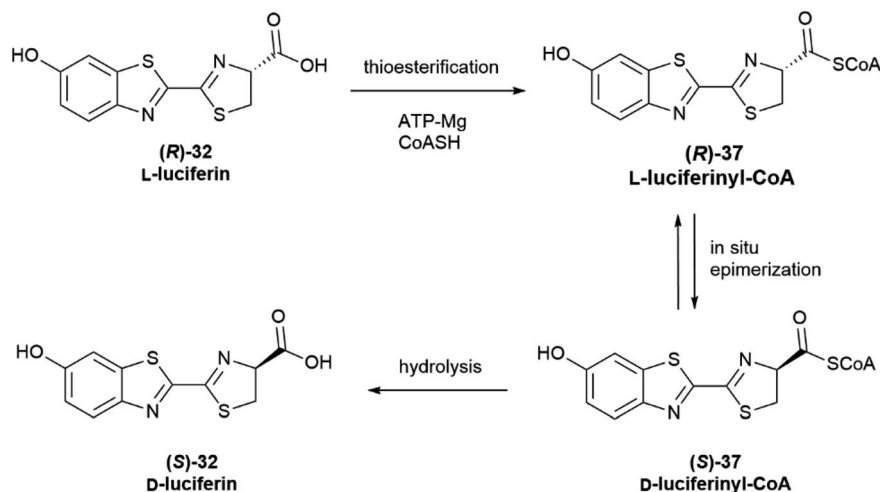
intensely sweet D-asparagine.<sup>60,61</sup> A sample of Piutti's *asparagina destrogira dolce* (dextrorotatory sweet asparagine) was recently discovered in the Schiff collection at the Florence Chemical Department.<sup>62</sup> Despite the popularity of this historical milestone of molecular chirality, the rationale for the production of sweet D-asparagine during germination of some legumes is unknown and puzzling, since seedlings do not tend to accumulate attractive, but rather deterrent (bitter or pungent) compounds. Also unknown are the metabolic fate of the non-proteinogenic version of asparagine and how the human sweet receptor, a T1R2 and T1R3 heterodimer which cannot distinguish between the enantiomeric forms of most sugars, can do so with the enantiomeric forms of asparagine.<sup>64</sup>

In most cases where the origin of the D-form of proteinogenic amino acids was investigated, specific racemases were shown to isomerize the corresponding L-isomer.<sup>56</sup> Most of these enzymes require pyridoxal 5' phosphate as cofactor, and isomerization occurs *via* reversible formation of a Schiff base with the 4-formyl group of pyridoxal and formation of an aza-quinoid intermediate.<sup>56</sup> However, other racemases, and specifically the bacterial version of glutamate and aspartate racemase, do not require a cofactor, and exploit cysteine residues for the deprotonation-riprotonation of the glutamate  $\alpha$ -position.<sup>56</sup>

Configurational inversion of proteinogenic amino acid generally precedes their incorporation in secondary metabolites, but partial racemization of the amino acid cysteine occurs during the biosynthesis of firefly luciferin. Bioluminescence is associated to the enzymatic production of luciferins, a class of



Scheme 5 Biosynthesis of D-luciferin (S)-32 in fireflies.



Scheme 6 Epimerization of luciferin in firefly and beetle.



compounds capable of light emission upon oxidation.<sup>65</sup> Firefly luciferin is a benzothiazole derivative [(*S*)-2-(6'-hydroxy-2'-benzothiazolyl)-2-thiazoline-4-carboxylic acid, (*S*)-32, *D*-luciferin, Scheme 4], which emits light with loss of CO<sub>2</sub> when oxidized by the enzyme firefly luciferase to form oxyluciferin 33.<sup>66</sup>

Only *D*-luciferin is recognized by the enzyme<sup>66</sup> and its oxidation is associated to the emission of light of pH-dependent maxima, but luciferin isolated from various insects is a scalemate, with the *D*-enantiomer dominating by a factor of *ca* 4 : 1.<sup>67</sup> *L*-Luciferin (*R*)-32 (Scheme 5) is the biosynthetic precursor of *D*-luciferin (*S*)-32, and is a strong inhibitor of firefly luciferase, interfering with the light-emitting reaction.

The first biosynthesis studies on luciferin from fireflies and beetles identified hydroquinone 34 and *L*-cysteine as its precursors, and later studies clarified the stereochemical aspects of the process (Scheme 5).<sup>68</sup> Hydroquinone 34 is oxidized to *p*-quinone 35, which undergoes thia-Michael addition of *L*-cysteine affording *L*-cysteinylhydroquinone (36), next turned into *L*-luciferin (*R*)-32 by reaction with a second molecule of *L*-cysteine in a yet mechanistically unclarified step.

The configurational inversion has been shown to occur in three steps (Scheme 6). The carboxylic group of *L*-luciferin (*R*)-32 is first enzymatically activated to the corresponding CoA

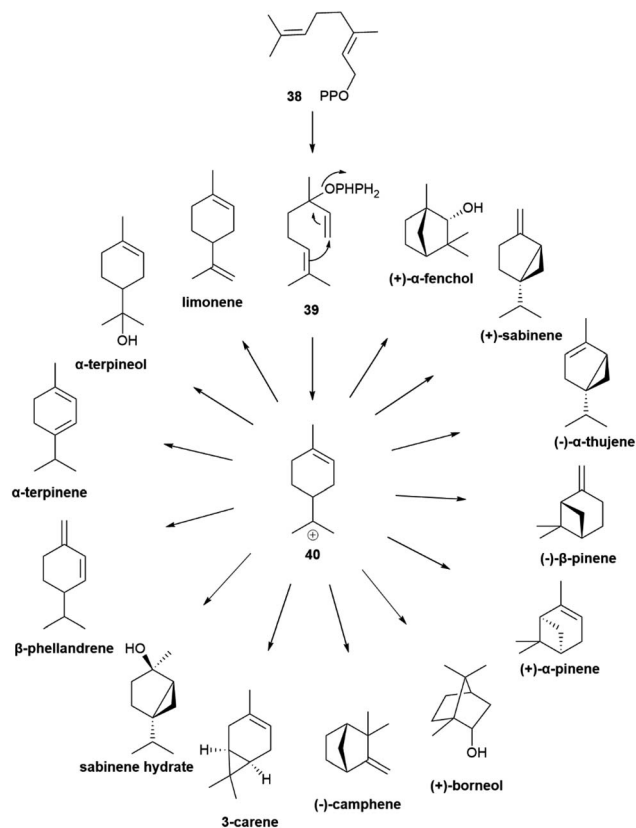
thioester (*R*)-37. This compound is configurationally unstable due to the increased acidity of the  $\alpha$ -carbon, and spontaneously enolizes, affording by re-protonation *D*-luciferyl-CoA (*S*)-37, next hydrolyzed to *D*-luciferin (*S*)-32.<sup>68,69</sup>

Noteworthy, luciferase appears to show different enzymatic activity for the two enantiomers, behaving as a thioesterase towards *L*-luciferin (Scheme 6) and as an oxidase towards *D*-luciferin (Scheme 4).<sup>65</sup> Moreover, *D*-luciferin inhibits the synthesis of *L*-luciferyl-CoA, and therefore self-limits its production, while an increased concentration of free *L*-luciferin inhibits the oxidation reaction, hindering the bioluminescence process.<sup>65</sup>

### 3.2 Co-expression of antipodal enzymes or directing proteins

**3.2.1 Polyene cyclization.** Monoterpene hydrocarbons are the archetypal class of scalemic natural products, since they rarely occur as racemates or in an enantiomerically pure form.<sup>70</sup> The scalemicity trait fades in higher isoprenoid classes, being rare in sesqui- and diterpene hydrocarbons, while, to the best of our knowledge, with a single exception,<sup>71</sup> antipodal triterpenoids have never been reported.<sup>72</sup> The biosynthesis of isoprenoids can be broadly divided into a cyclase and an oxidase phase.<sup>73</sup> In the biosynthesis of lower (C10–C15) isoprenoids and some diterpenoids, the cyclase phase generates a cyclic framework by displacement of an electrophilic diphosphate precursor with a trisubstituted nucleophilic double bond, as exemplified by the generation of the  $\alpha$ -terpinyl cation (40) from linalyl pyrophosphate 39, originating in turn from geranyl pyrophosphate 38 (Scheme 7).

The cyclic cationic 40 can then undergo distinct rearrangements, and is eventually quenched by proton loss or water trapping (Scheme 7). In the oxidase phase, the primary skeletons are then decorated with oxygen functionalities which, in turn, can trigger additional ring rearrangements and closures that significantly expand skeletal diversity. The oxidase phase relies on cytochrome P450 monooxygenases that show high substrate enantiospecificity,<sup>73</sup> and effectively upgrade the enantiomeric purity of their hydrocarbon substrates. With the notable



Scheme 7 Monoterpenes derived from the *para*-menthane cation 40. For compounds having multiple stereocenters, the configuration of the more common enantiomer was depicted (ROMPP Lexicon, Thieme Verlag, 1997).

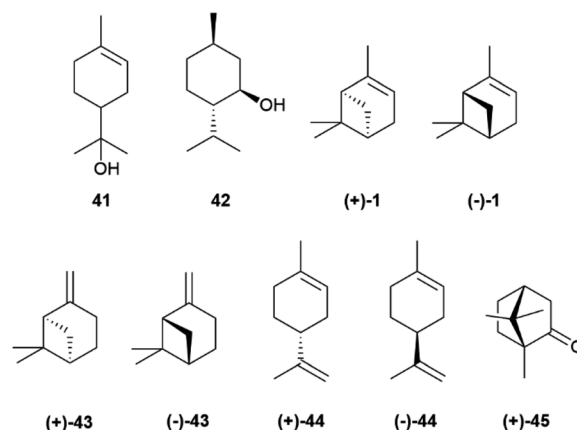


Fig. 8 Structure of chiral monoterpenes 41–45 and 1.

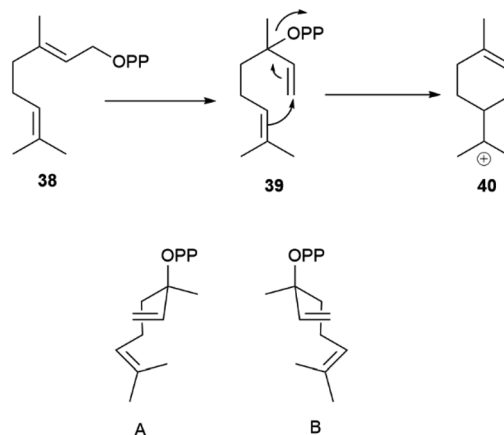


exception of alcohols, like  $\alpha$ -terpineol (**41**, Scheme 7 and Fig. 8), directly generated from a cyclase primary cation by water trapping, the cyclic monoterpene alcohols show very high optical purity, as exemplified by menthol (**42**, Fig. 8).<sup>70</sup> The cyclase phase in the biosynthesis of triterpenoids is of the cascade-type, and is triggered by protonation of a double bond or an epoxide rather than by ionization of a pyrophosphate. However, this difference alone does not explain the enantiomeric purity of these compounds, since the cascade cyclization mode can also operate in diterpenoids, where it can generate enantiomeric forms.<sup>72</sup> The occurrence of triterpenoids in a single enantiomeric form could perhaps be traced to the high genomic burden associated to building enantiomorphous active sites for large substrates. Thus, it may not be by chance that antipodal monoterpene synthases recognize enantiomeric substrate folds,<sup>74</sup> while enantiodivergence associated to antipodal sesquiterpene synthases exploits differences in reaction mechanism (see *infra*).<sup>75</sup>

The enantiomeric composition trait of monoterpene hydrocarbons differs greatly even between closely related compounds. Thus, while (+)- $\alpha$ -pinene ((+)-**1**, Fig. 8), (-)- $\beta$ -pinene ((-)-**43**) and (+)-limonene ((+)-**44**), can be isolated in large amounts and with ee around or even higher than 90%, their enantiomers ((-)-**1**, (+)-**43** and (-)-**44**, respectively) are only available in lower amounts and optical purity.<sup>70</sup> The optical purity of pinenes can be upgraded (see Section 4), and they can serve as starting material for the synthesis of other enantiopure terpene hydrocarbons, including (-)-limonene ((-)-**44**), scarcely available by isolation (Fig. 8). Since many oxygenated monoterpenes are crystalline, the cheap scalemic form of the “big three” can be used to prepare oxygenated terpenes. Indeed, most camphor (**45**) on the market is nowadays obtained not by isolation but by synthesis from natural  $\alpha$ -pinene.<sup>70</sup>

Many monoterpene synthases have been cloned and heterologously expressed in bacteria and yeasts.<sup>75</sup> However, yields have so far remained significantly lower than those achieved for hemiterpenes and sesquiterpenes, some of which can be obtained by fermentation in transgenic organisms in two- or even three digit mg yields per liter.<sup>76</sup>

The scalemic state of monoterpene hydrocarbons is generally due to the co-expression of antipodal synthases,<sup>74</sup> and more rarely to the generation of uneven ratios of both enantiomers by the same cyclase.<sup>77</sup> All monoterpene synthases share a mechanism based on the ionization of a linear isoprenyl diphosphate by a trinuclear magnesium(II) cluster bound to an aspartate-rich motif (DDXD) in the active site, a feature generally conserved in plant, microbial and fungal isoprenoid synthases.<sup>77</sup> The cation is then trapped, in a head to tail fashion, by the distal double bond, generating a cationic species that can be directly quenched by proton loss or water trapping (Scheme 7). Alternatively, the cation can undergo one of more sequences of Wagner–Meerwein rearrangement or of hydride shift before the termination step.<sup>77</sup> Cyclases are not generally highly selective in the termination step and, therefore, at directing the biosynthetic flux down one specific reaction manifold. Thus, half of the known terpene cyclases generate, in addition to a main



Scheme 8 Head-to-tail cyclization of geranyl diphosphate (**38**) via enantiomeric folds (A and B, 3aR and 3aS, respectively) of linalyl diphosphate (**39**).

reaction product, a constellation of additional products which generally makes up >10% of the reaction mixture.<sup>77</sup>

Geranyl pyrophosphate (**38**, Scheme 8) cannot cyclize directly, since the interaction of its cationic head with the nucleophilic terminal double bond of the substrate would generate an *E*-cyclohexene. Therefore, isomerization to linalyl pyrophosphate (**39**) and next to a linalyl cation **40** must take place in the course of the reaction, leading to two enantiomeric helical conformations A and B (Scheme 8) for the achiral linalyl cation precursor. Alternatively, but much more rarely, the cyclase can directly recognize a neryl pyrophosphate substrate, like in tomato glandular trichomes.<sup>76</sup>

Generally, only a single *cisoid anti-endo* fold is recognized by the cyclase (Scheme 8). Therefore, when more than one constitutional isomer is generated by distinct termination steps, only monoterpenes belonging to the same configurational series are formed.<sup>76</sup> Thus, the (-) limonene synthase from *Abies grandis* (Douglas ex D. Don) Lindl. in addition to (-)-limonene ((-)-**44**) also produces (-)- $\alpha$ - and (-)- $\beta$ -pinenes ((-)-**1** and (-)-**43**, respectively), all three compounds deriving from the same (*S*)-menthenyl cation ((*S*)-**40**).<sup>78</sup> Exceptions are, however known, and some terpene cyclases produce scalemic cyclic terpenes or mixtures of cyclic terpenes derived from different folds of the linalyl precursor.<sup>77</sup> Remarkably, terpene synthases with different enantioselectivity can be co-expressed. Thus, from the loblolly pine (*Pinus taeda* L.), a major pulpwood species and the most common tree species in US after red maple,<sup>79</sup> two enantioselective (+) and (-)- $\alpha$ -pinene synthases were cloned, while the  $\alpha$ -terpineol synthase from the same source plant produced a scalemate, with only ca 80% enantiomeric excess.<sup>74</sup> The two antipodal  $\alpha$ -pinene synthases from the loblolly pine show relatively low level (75%) of sequence homology, suggesting that they diverged from a common ancestor long ago.<sup>74</sup> Modifications of chemoselectivity in terpene synthases require the change of only a few amino acids, but the sequence differences between the two antipodal  $\alpha$ -pinene synthases shows that the alteration of substrate enantioselectivity has a much higher genomic cost.<sup>74</sup>



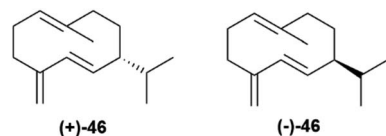
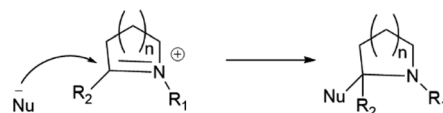


Fig. 9 Structure of the two germacrene D-enantiomers.

Germacrene D synthase is the best characterized case of differently co-expressed antipodal and enantioselective terpene synthases.<sup>75,80</sup> Germacrene D (**46**, Fig. 9) is an important intermediate in sesquiterpene biosynthesis, and occurs across a wide range of organisms, from bacteria to liverworts and plants. The (+)-enantiomer ((+)-**46**) is typical of lower organisms, while most plants produce the (–)-enantiomer ((–)-**46**).<sup>80</sup>

Asteraceous species from the genus *Solidago* are an exception, since they produce both enantiomeric forms of germacrene D in a ratio which depends on season, location and plant part investigated, with an almost racemic state detected in most accessions analyzed.<sup>81</sup> Two antipodal germacrene D synthases were characterized from *S. altissima* L. (tall goldenrod), and, by using deuterium-labelled substrates, it was shown that they differ in the mechanism of charge propagating step.<sup>75,80</sup> Both enzymes generate an 11-germacradienyl cation (**48**, Scheme 9) by intramolecular interaction between the electrophilic diphosphate site and the nucleophilic  $\omega$ -double bond of farnesyl pyrophosphate (**47**, Scheme 9), and both enzymes form the  $\Delta^{5(15)}$  exomethylene by proton loss from the allylic C-15 methyl of a C-6 germacra- $\Delta^{1(10),5}$ -dienyl cation (**48**, Scheme 9). However, the propagation step in the (–)-germacrene D synthase involves a 1,3 anionic shift of the  $\beta$ -C-6 hydrogen to C-11 (Scheme 9b), while the formation (+)-germacrene D (+)-**46** involves a sequence of two 1,2-hydride shifts, the first one from the  $\alpha$ -hydrogen at C-7 to C-11, and the second one of the  $6\beta$ -hydrogen to C-7 (Scheme 9a). As a result of the different shift of the  $6\beta$ -hydrogen, the two enantiomeric germacrene D are formed. Both *Solidago* germacrene D synthases were cloned, and showed a remarkable sequence identity, as expected for a mechanism of enantio-divergency based on a reaction course rather than on the recognition of enantiomeric chiral substrate folds.<sup>80</sup>

**3.2.2 Iminium ion trapping.** While pelletierine (**14**, Fig. 4) is generated in an enantiomerically pure form and then



Scheme 10 Biogenetic derivation of pyrrolidine ( $n = 1$ ) and piperidine ( $n = 2$ ) alkaloids.

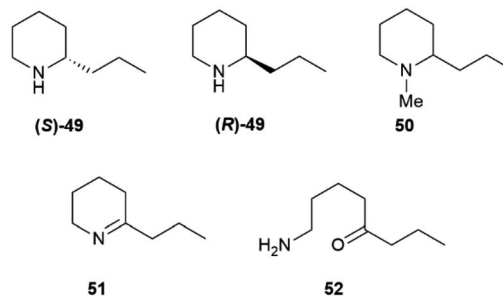
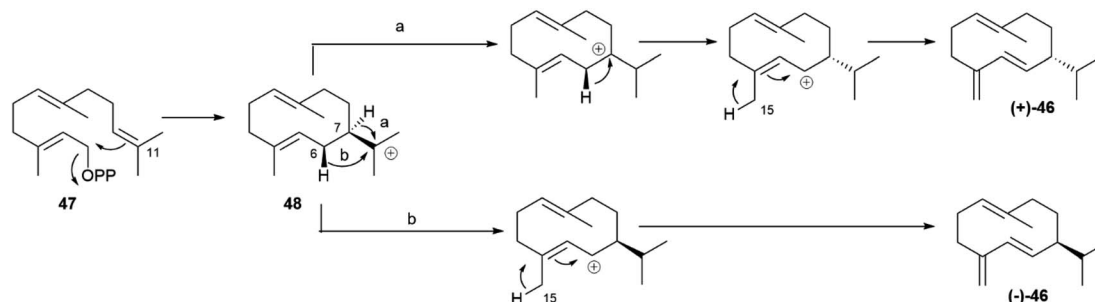


Fig. 10 Structures of piperidine alkaloids **49–51** and their precursor **52**.

spontaneously racemizes, some biogenetically related, and configurationally stable, bioactive piperidine and pyrrolidine alkaloids are isolated as scalemates or racemates.<sup>82</sup> These alkaloids derive from nucleophilic attack of a ketide anion or of a NADP-derived hydride equivalent to an iminium ion (Scheme 10), and enantiomorphic enzyme cavities, equivalent of the enantiomorphic terpene cyclases, are seemingly involved in their biosynthesis. The iminium ion can be derived from a basic amino acid ( $R_1 = \text{Me}$ ,  $R_2 = \text{H}$ ) or from a ketide construct ( $R_1 = \text{H}$ ,  $R_2 = \text{alkyl group}$ ).

Some of these alkaloids and pseudoalkaloids are of significant relevance for toxicology and our cultural history. Coniine, the poisonous principle of spotted hemlock (*Conium maculatum* L.), was the first “alkaloid” to be structurally elucidated (Hofmann, 1881)<sup>83</sup> and synthesized (Ladenburg, 1886).<sup>84</sup> Coniine **49** and its *N*-methyl derivative (**50**), that actually are pseudoalkaloids, are scalemic, with a prevalence of the (*S*)-(+)-enantiomer ((*S*)-**49**) (Fig. 10).<sup>85</sup> Coniine binds to the nicotinic acetylcholine receptor (nAChR), activating and eventually blocking it, with depolarization of post synaptic neuromuscular junctions and flaccid paralysis.<sup>85</sup> The pharmacological potency



Scheme 9 Mechanism for the enantioselective formation of (+)- and (–)-germacrene D ((+)-**46** and (–)-**46**, respectively) by antipodal germacrene D synthases.



of coniine enantiomers is different, with the (*R*)-(-) enantiomer ((*R*)-49) outperforming the (*S*)-(+) enantiomer ((*S*)-49) in terms of both cholinergic activity (one order of magnitude) and overall acute toxicity (murine LD<sub>50</sub> 7 mg vs. 12 mg kg<sup>-1</sup> by IV administration in mice).<sup>85</sup> Chronic administration of sub-lethal dosages of coniine is associated to teratogenic effects, and it has been suggested that the major toxicity of (*R*)-(-) coniine ((*R*)-49) is retained also in terms of chronic effects.<sup>85</sup> The toxicological relevance of coniine is not only historical (Socrates's death sentence was carried out with hemlock juice), since it is still associated to cattle loss and to human fatalities, both by direct consumption of the plant<sup>86</sup> and *via* the food chain. Thus, coniine is not toxic for quails (*Coturnix coturnix* coturnix), and possibly also some other birds, which can impudently eat its seeds and store the alkaloid in their flesh.<sup>87</sup> The consumption of quails can be associated to severe toxicity (coturnism) with death and rhabdomyolysis in severe cases.<sup>87</sup> Quails also feed on other toxic plants like henbane and water hemlock, and thus coniine could be only one of the toxic cocktail accumulated by these birds. The involvement of a hereditary enzyme deficiency has also been suggested to play a role, but no specific enzyme has yet been identified.<sup>87</sup> Coniine originates from the NADPH-dependent reduction of achiral  $\gamma$ -conicein (51) by a specific reductase.<sup>88</sup> In turn,  $\gamma$ -conicein originates from 52, the reductive transamination product of 5-oxooctanal, a polyketide construct.<sup>89</sup> The transcriptome sequencing of coniin biosynthesis in *C. maculatum* has been reported, and eight transcripts for  $\gamma$ -conicein reductase were identified.<sup>89</sup> However, additional studies to validate the candidates' function and confirm their role *in planta* have not yet been carried out, and therefore the presence of functionally distinct forms of the enzyme needs confirmation. Coniine-type alkaloids also occur in plants unrelated to hemlock: seven carnivorous species of the genus *Sarracenia* and twelve *Aloes* have been reported to contain these alkaloids.<sup>90</sup> It has been speculated that *S. flava* uses coniine to paralyze its insect preys, but the enantiomeric composition of coniin in these plants is not known.

Nicotine (*S*)-7, at least when isolated from tobacco leaves, can be considered almost optically pure due to the selective demethylation of the *R*-enantiomer ((*R*)-7, Fig. 1) described in the introduction. On the other hand, its related minor tobacco

alkaloids are scalemic [nornicotine (53) and anatabine (54)] or almost racemic [anabasine, 8] (Fig. 11).<sup>91,92</sup>

Overall, the issue of chirality seems to have been largely overlooked also in the study of the genomics and enzymology of pyridine alkaloid biosynthesis, one contributing reason being the contrasting literature data on their enantiomeric composition, possibly related to SDE associated to the volatility of these alkaloids. Tobacco alkaloids are all structurally similar, but can have different biogenetic origin.<sup>91,92</sup> Nicotine (*S*)-7 and anabasine 8 derive from the convergence of the diamine and the NADPH pathways (Scheme 11) and only differ for the starting amino acid precursor.

On the other hand, anatabine (54) derives from the dimerization of two nicotinic acid-derived dihydropyridine intermediates, and nornicotine (53) from the demethylation of nicotine.<sup>91</sup> Chirality is associated to the formation of the dinuclear system, and different versions of the coupling enzyme seemingly exist. Also puzzling is the racemic state of anabasine (8) in the leaves, which sharply contrasts with the optical purity of nicotine. Anabasine is a potent teratogen, and is the major alkaloid of *Nicotiana glauca* L., where it occurs as a scalemate.<sup>92</sup> The teratogenic alkaloid ammodendrine (55, Fig. 11) from various lupin (*Lupinus* spp. vv.) species is biogenetically related to anatabine, and is also scalemic.<sup>92</sup>

Intermolecular iminium ion trapping can also be at the origin of scalemate formation, as exemplified by a series of dihydrobenzophenanthridine alkaloids from celandine (*Chelidonium majus* L.) of general formula 56 (Scheme 12), derived from nucleophilic addition to a 5,6-iminium ion 57. The nucleophilic species is derived from an acetate unit 58 *via* enolization or from a thiamine-associated umpolung synthon 59.<sup>93</sup>

**3.2.3 Radical coupling.** A large number of scalemic natural products are the result of copper-based (laccase) oxygenase activity or, alternatively, of iron-based oxygenase strategies where the first half-reaction (generation of a phenoxy radical by a high-valency oxoiron oxidant) is not accompanied by hydroxyl radical transfer *via* a classic rebound mechanism. These

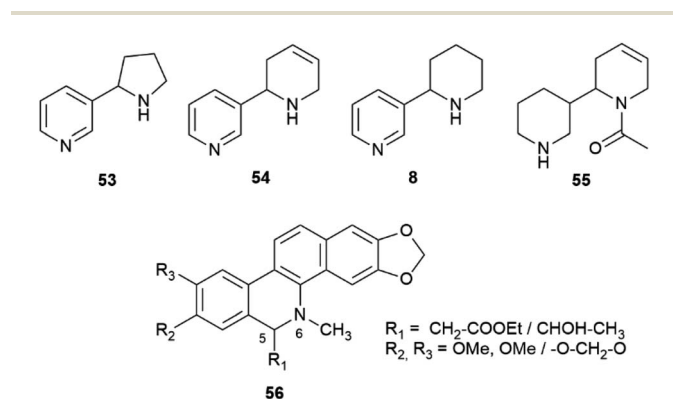
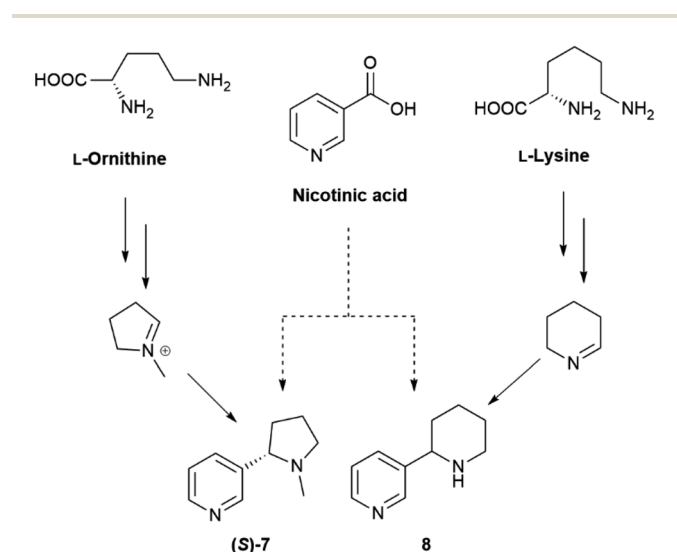
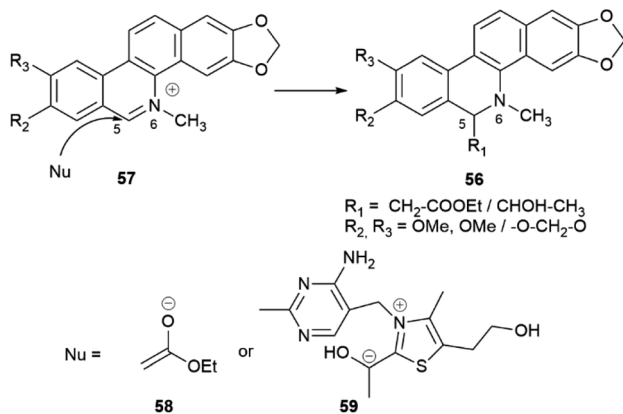


Fig. 11 Structures of "minor" tobacco alkaloids (53, 54, 8, 55) and of the benzophenanthridine alkaloids of general formula 56.



Scheme 11 Biosynthesis of nicotine (*S*)-7 and anabasine 8.





Scheme 12 Non-enantioselective formation of alkaloids of general formula 56.

phenoxy radicals last long enough to pair and couple through different resonance contributors, resulting in alkyl-alkyl coupling or, alternatively, into aryl-aryl coupling.

**3.2.3.1 Alkyl coupling.** The monoelectronic oxidation of alkenylphenols by laccases and related oxygenases generates stabilized radicals that can couple with different regio- and stereo-chemical results. Of particular relevance is coupling at the distal alkyl carbon, since it is involved in the generation of the complex polymer lignin as well as of lignans, a class of C6-C3 dimers of wide distribution in plants. While lignin is racemic, lignans originating from this coupling, as well as their reductive cleavage products, are generally obtained as scalemates by isolation, and only more rarely as optically pure or racemic species. The oxidative dimerization of the monolignol *E*-coniferyl alcohol (60, Scheme 13) to the furofuran pinosresinol (61), and the subsequent stepwise reduction to the furan lariciresinol (62) and the dibenzylbutane secoisolariciresinol (63) exemplify the early steps of lignan biosynthesis.<sup>94,95</sup> The principal isomers isolated from *Forsythia intermedia* are depicted in Scheme 13. However, the compounds are generated in variable enantiomeric composition, depending on several factors.

The products of further downstream biogenetic oxidative elaboration are generally enantiomerically pure, as exemplified by podophyllotoxin (64). Thus, while pinosresinol (61) occurs in

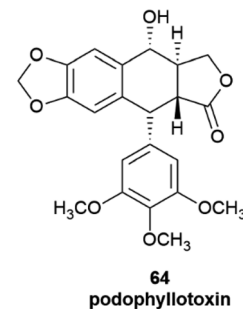
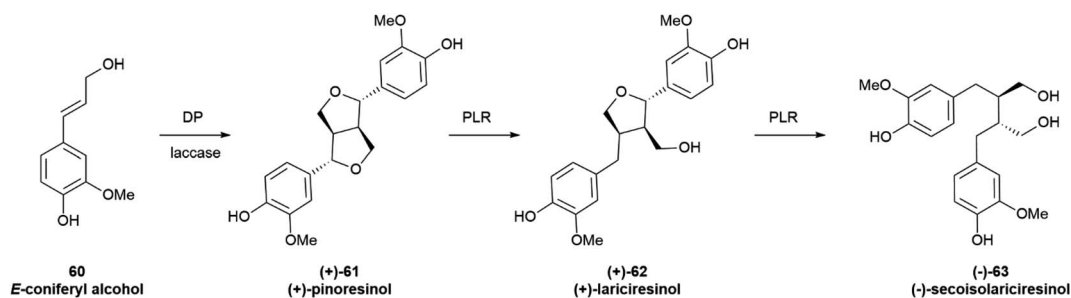


Fig. 12 Podophyllotoxin 64.

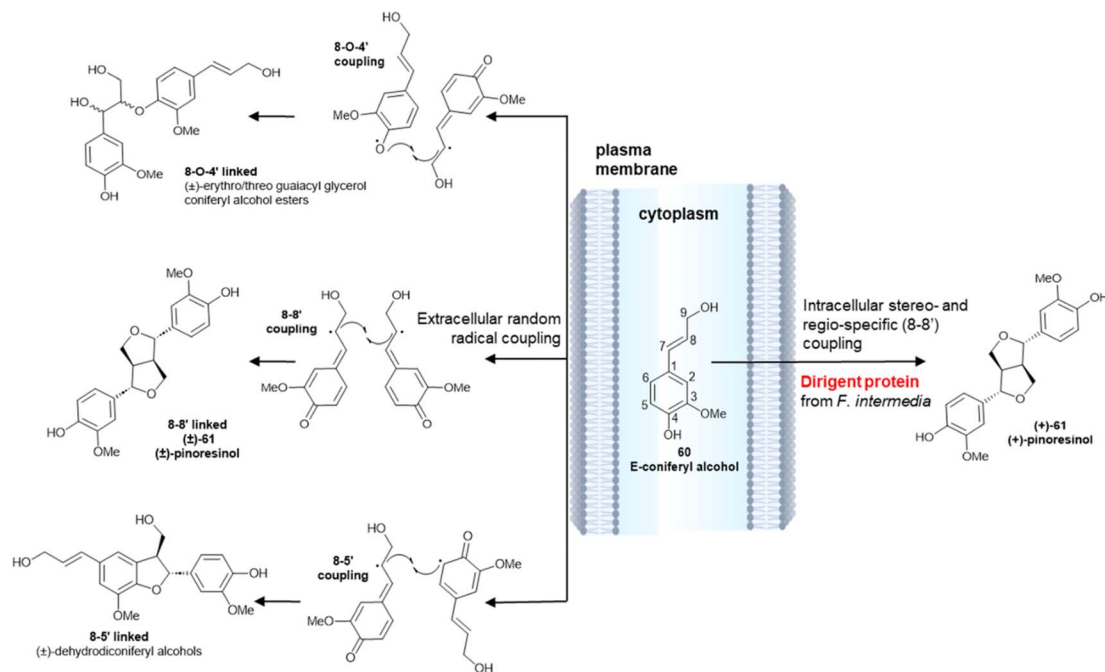
scalemic forms of opposite enantiodominance even within same plant, the same enantiomeric form of podophyllotoxin (64, Fig. 12) and its analogues have been isolated in enantiopure form in not less than nine distinct and taxonomically unrelated plant families.<sup>96</sup>

The different enantiopurity of lignin and lignans is related to the cellular milieu where the monoelectronic oxidation takes place. The dimerization of monolignol, as exemplified by coniferyl alcohol (60) is initiated by a single-electron transfer catalysed by a laccase or a peroxidase (Scheme 14). The resulting delocalized radical has three distinct coupling modes, and can generate 8-*O*-4', 8-8' or 8-5' linked dimers.<sup>97</sup> The bis-quinonmethide generated in the 8-8' coupling step next undergoes a double intramolecular oxa-Michael addition, eventually generating a diaryl furofuran system (61). Coupling outside the cell membrane is regio- and stereo-random (Scheme 14, left), generating an achiral polymer (lignin) where all three types of coupling are represented. Conversely, intracellular coupling is chemoselective, and leads regioselectively to dimers (monolignols) that originate only from 8-8' coupling and have a variable degree of enantiopurity (Scheme 14, right). This remarkable difference has been related to the association of the oxidizing enzyme(s) with specific non-enzymatically active cytoplasmatic proteins, that have been named Directing Proteins (DP).<sup>98</sup> These ubiquitous proteins bind the reactive radicals generated by the oxidase enzymes, fluxing them into distinct coupling manifolds.



Scheme 13 Oxidative coupling of *E*-coniferyl alcohol (60) to the furofuran lignan pinosresinol (61) is followed by stepwise reduction to lariciresinol (62) and to secoisolariciresinol (63). DP = Dirigent protein, PLR = Pinosresinol-lariciresinol reductases. The major isomers isolated from *Forsythia intermedia* are depicted. However, the compounds are generated in variable enantiomeric composition depending on several factors detailed in the text.





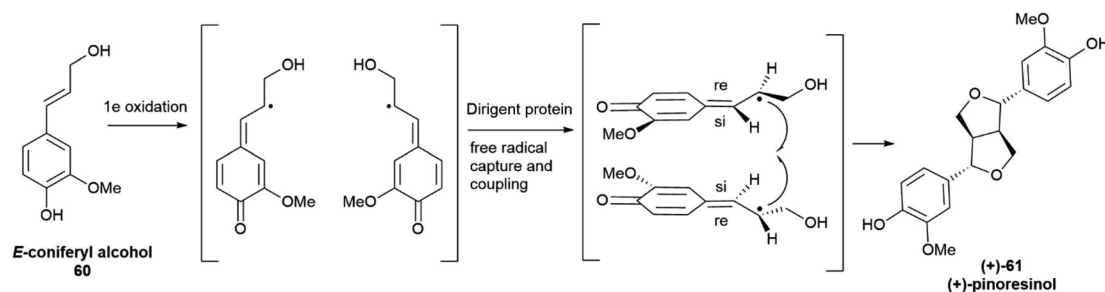
Scheme 14 Random radical coupling of *E*-coniferyl alcohol **60** vs. stereo- and regio-specific intracellular coupling in the presence of a Dirigent Protein from *Forsythia intermedia* (ref. 98).

The seminal discovery of DP was reported in 1997 as a result of extensive studies on the biosynthesis of lignans in plants from the genus *Forsythia*, a prolific producer of 8,8'-lignans. Using *in vivo* tracer labelling studies, the formation of (+) pinoresinol ((+)-**61**, Scheme 15) was investigated in cell cultures and in cell-free extracts of the plant, using hydrogen peroxide as a cofactor. The formation of (+)-**61** involved the cooperation of two proteins, only one of which, a laccase, endowed with enzymatic activity. The second protein did not affect the rate of the one-electron oxidation step, rather it appeared to bind the laccase generated radical to secure regio- and enantioselectivity of the coupling step.<sup>98,99</sup> When the reaction was carried out with the laccase alone, a complex mixture of racemic isomers was generated, highlighting the key role of DP to steer in a regio- and enantioselective fashion the coupling reaction.

DP showing opposite enantioselectivity relative to the one described in *Forsythia* were characterized from other plants.<sup>100</sup> Crystal structures were obtained for the DPs associated to the

generation of (+) pinoresinol ((+)-**61**) in *P. sativum* (PsDRR20) and of (–)-pinoresinol ((–)-**61**) in *Arabidopsis thaliana* L. (PsDRR20 and AtDIR6, respectively).<sup>101</sup> Both proteins are eight-stranded antiparallel β-barrel trimers, and present two-lobed cavities with adjacent binding sites to accommodate a pair of coniferyl alcohol radicals in an orientation suitable for the 8–8' coupling. One DP favours coupling at the *si-si* faces, and the other one at the *re-re* face of the interacting radicals, leading to (*R,R*)- or (*S,S*)-bisquinonmethides, and next to (+) or (–)-pinoresinol.<sup>102</sup>

Despite the existence of enantioselective DPs, pinoresinol occurs in many plants as a scalemate,<sup>94</sup> presumably because of the presence of antipodal DPs, or because of a suboptimal production of a single DP and a kinetic mismatch between the rate of radical generation by the laccase and the rate of radical trapping by the DP. Different organs of the same plant can also contain different enantiomers of pinoresinol, due to the expression of distinct DPs. Thus, burdock (*Arctium lappa* L.)



Scheme 15 Directing protein-mediated oxidative coupling of the monolignol **60** (coniferyl alcohol) into (+)-pinoresinol (+)-**61** in *Forsythia intermedia*.



contains the (+)-enantiomer (+)-**61** in petioles and the (–)-enantiomer (–)-**61** in the seeds.<sup>103</sup> Environmental factors also play a role, since DPs are thermolabile, and are inactivated by temperatures >33 °C.<sup>104</sup> The erosion of enantiomeric purity due to a suboptimal concentration of DP is also associated to a reduction of regioselectivity, with generation of other types of couplings (8–5′- and 8–O–4′).<sup>104</sup>

The furofuran system of the primary coupling product pinosresinol next undergoes reductive cleavage, with formation of monocyclic and then acyclic derivatives (**62** and **63** in Scheme 13, respectively). In this way, the furan-type lignan lariciresinol (**62**) and the dibenzyl-type lignan secoisolariciresinol (**63**) are generated from the furofuran lignan pinosresinol (**61**) through the agency of the NADPH-dependent pinosresinol/lariciresinol reductase (PLR). Two isoforms of this enzyme have been characterized, displaying opposite enantioselectivity.<sup>105</sup> The enantiomeric ratio of the starting pinosresinol is significantly affected by the agency of these two reductases, which show various degrees of enantioselectivity toward their substrates and different levels of expression in different plant tissues. Thus, pinosresinol reductase kinetically resolves its scalemic (–)-substrate in the seeds of *A. lappa* L., but significantly erodes the enantiomeric excess of scalemic (–) pinosresinol in *Wikstroemia sikokiana* Franch. & Sav. and in *Forsythia koreana* (Rehder) Nakai.<sup>106</sup> Similarly, lariciresinol reductase from *F. koreana* upgrades the enantiomeric excess of its substrate, generating (–)-secoisolariciresinol (–)-**63** in >99% ee from a highly scalemic (–) lariciresinol (ee ca 35%). In contrast, the lariciresinol reductase in the seeds of *A. lappa* L. significantly erodes the optical purity of its substrate, generating (–)-secoisolariciresinol of 38% ee from optically pure (–) lariciresinol.<sup>106</sup>

In summary, furofuran lignans and their products of reductive cleavage are a major class of scalemic natural products. The scalemic state is primarily associated to a suboptimal involvement of Dirigent proteins in the oxidative coupling of the monolignol precursor, but the enantiomeric composition can be significantly affected by the activity of reductases *en route* to monofuran and dibenzylbutane lignans. The further oxidative modification of these compounds is instead associated to the activity of highly enantioselective oxidizing enzymes, and aryl-tetralin lignans and other biogenetically downstream lignans are generally isolated in enantiomerically pure form.

Little systematic attention has been given to the enantiomeric composition of neolignans, the result of 8–5′ coupling of the quinonmethide radicals (Scheme 14), but it has been suggested that the scalemic state discovered in gardenifolin A (**65**, Fig. 13) and related compounds from *Gardenia ternifolia* could

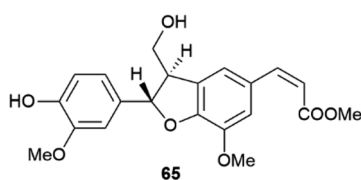
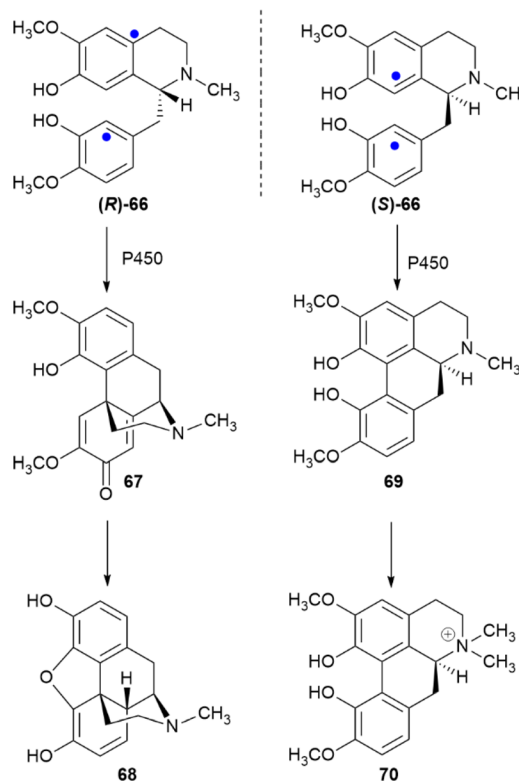


Fig. 13 Structure of gardenifolin A **65**.

be widespread, or even the norm within this class of compounds.<sup>107</sup>

**3.2.3.2 Aryl coupling.** Biaryl coupling is involved in the biosynthesis of compounds from different classes, and one could cogently argue that the presence of an electron-rich aryl moiety is an irresistible invitation for Nature to expand the diversity of secondary metabolites. In the presence of a directing stereocenter, coupling can be highly regio- and enantioselective. Thus, under the agency of specific P450 oxidases,<sup>108</sup> the two aromatic moieties of the benzyloquinoline alkaloid (*R*)-reticuline ((*R*)-**66**) couple in an *ortho-para* fashion to salutaridin (**67**) *en route* to morphine (**68**), while in (*S*)-reticuline ((*S*)-**66**) they couple in an *ortho-ortho* fashion to corytuberine (**69**), *en route* to magnoflorine (**70**) (Scheme 16).<sup>108</sup>

In the absence of directing stereocenter(s), aryl coupling is more “plastic” and can generate enantiomerically pure compounds, racemates or scalemates, depending on the specificity of the oxidase involved and/or the involvement of dirigent proteins. The enantiomeric state of chiral biphenyls and their derivatives is, in any case, complex, since a low enantioselectivity in the coupling step leading to a scalemic mixtures of atropisomers can be followed by enantioselective reactions (oxidations or glycosidations), while the presence of aromatic rings facilitates racemization reactions associated to the configuration of benzylic/vinylic positions. Chiral neolignans containing a biphenyl system are generally racemic or scalemic, but the involvement of directing proteins in their biosynthesis is unclear. Remarkably, both atropisomers are retained even



Scheme 16 Enantiodivergent metabolic role of reticuline (**66**). The sites of aryl coupling are indicated by blue dots.





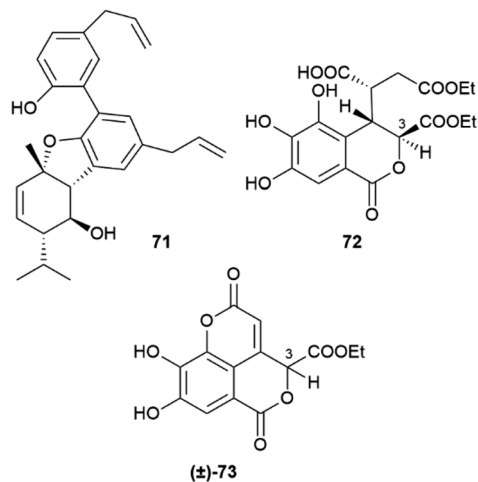
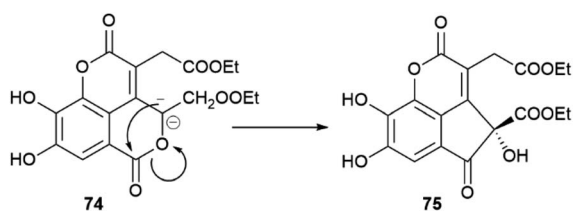


Fig. 14 Structure of magmentane A 71, euphorhirtin F 72, euphorhirtin H 73.

after further elaboration, including not only hydroxylation but also combination with monoterpenes with stereogenic centers, like in magmentanes (*e.g.* magmentane A, 71, Fig. 14) from *Magnolia officinalis* L.<sup>109</sup> In compounds derived from the degradation of axially chiral phenolics, biogenetically closely related and co-occurring compounds can show a surprisingly different optical purity, as shown by the chebulic acid derivatives of *Euphorbia hirta* L.<sup>110</sup> In this plant, various enantiopure esters of the degraded biphenyl chebulic acid (*e.g.* euphorhirtin F, 72, Fig. 14) occur along with their racemic coumarinic analogues (*e.g.* euphorhirtin H [(±)-73, Fig. 14]) from which, however, the scalemic rearranged cyclization product 75 (euphorhirtin L) is derived by an intramolecular Claisen condensation (Scheme 17). The racemic state of the coumarin derivatives might be associated to the increased acidity of C-3, a vinylogous  $\alpha$ -carbonyl position, while the scalemic state of the rearranged compound could result from the activity of enantio-discriminating enzyme(s). Interestingly, the scalemic state of 75 was suggested by a crystal analysis, which showed a spatial group (P1) typical of a scalemate.<sup>110</sup> Chiral phase HPLC next confirmed the presence of a 1 : 3 mixture of enantiomers in the optically active natural product,<sup>110</sup> and one wonders how many chiral “biaryloids” assumed to be enantiopure actually deserve this status.



Scheme 17 Enzymatic conversion of a racemic coumarin-type euphoritin 74 into scalemic euphorhirtin L (75) by intramolecular Claisen condensation.

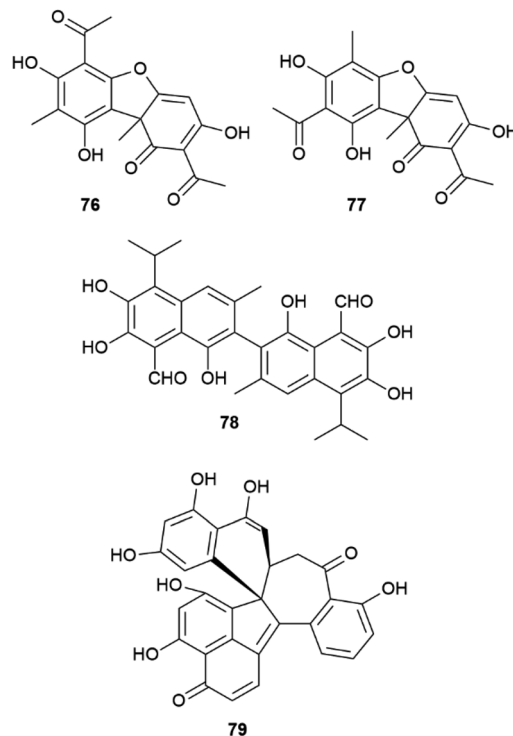


Fig. 15 Structure of usnic acid (76), iso-usnic acid (77), gossypol (78), dalesconol C (79).

Another remarkable example of the plasticity of aryl coupling is usnic acid (76, Fig. 15), the archetypal lichen constituent. This compound can occur in both enantiopure forms, as a scalemate, or as a racemate depending on the lichen species.<sup>111</sup> In addition, some lichens also contain iso-usnic acid (77), a signature of a non-regioselective coupling.<sup>111</sup> Usnic acid used to be a popular ingredient in weight-loss products, but was later banned by FDA because of its association to severe liver damage.<sup>112</sup> Remarkably, the huge toxicological literature on the hepatotoxicity of usnic acid often ignores its stereochemical diversity. Since the biological profile of the two enantiomers is not overlapping,<sup>113</sup> one wonders if some controversial aspects of the toxicity profile of usnic acid could actually be related to the study of samples having a different enantiomeric composition.

Also the binaphthyl gossypol (78) shows a different distribution in the cotton plant in terms of enantiopurity. Depending on the cotton variety or of the *Gossypium* species, scalemic forms with different dominant enantiomers have been described, with the (+) atropisomeric form generally prevailing.<sup>114</sup> A specific dirigent protein (GhDIR4) has been described to confer atroposelectivity to hemigossypol coupling in the presence of laccase and oxygen.<sup>115</sup> GhDIR4 was the second dirigent protein to be discovered and cloned, providing support to the general involvement of these agents in oxidative coupling reactions, not only in lignans biosynthesis.<sup>115</sup> The laccase-promoted dimerization of hemigossypol to gossypol in the presence of GhDIR4 p reduces (+)-gossypol in more than 80% ee. The (–) enantiomer prevails in some *Gossypium* species, but



characterization of the directing protein from these plants could not be carried out.<sup>115</sup>

For complex phenolics, the generation of scalemic products of aryl coupling does not depend on directing proteins, but could be related to conformational preferences of the intermediate radicals, as suggested for dalesconol C (79, Fig. 15) and related tri-naphtyls.<sup>116</sup> Different helicities of the reacting radical(s) could be recognized differently in terms of  $\pi$ - $\pi$  interactions by the active site of laccases, affording a scalemate whose composition depends, assuming a kinetic control, on the relative conformational stability of the radical substrate(s). This concept is, in principle, of general relevance, and worth of a systematic investigation.

Within compounds whose chirality is associated to biaryl coupling, the anticancer alkaloid cephalotaxine (5, Scheme 18) presents an additional interesting case. Depending on the *Cephalotaxus* species, cephalotaxine can be isolated both as enantiopure or scalemic, a surprising observation since this compound features three stereogenic carbons.<sup>7</sup> A possible explanation can be found in the stereocontrol exerted by the stereocenter C-1 of the isoquinoline 80 over the phenol coupling that ultimately generates 81 and the subsequent cascade of events leading to cephalotaxine. Thus, after *ortho-para* coupling and cleavage of the 1-8a bond, the chiral dibenzo azacyclodecane 81 could stereospecifically undergo hydride abstraction coupled to nitrogen trapping (82) and afford the spirane 83, which is next converted into cephalotaxine 5 by a decarboxylative benzylic acid rearrangement and alkylative modification of the phenolic hydroxyls.<sup>117</sup> If this entire process is ultimately controlled by the configuration of carbon C-1 in 80, the different enantiomeric purity of cephalotaxine from different sources relates back to stereocontrol in the generation of this stereocenter.

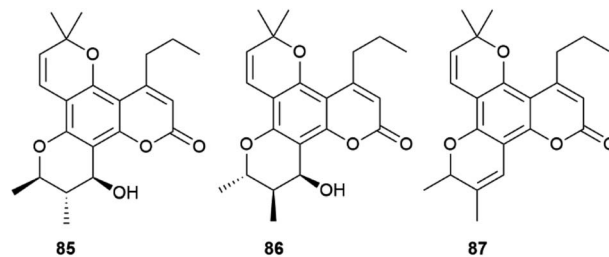
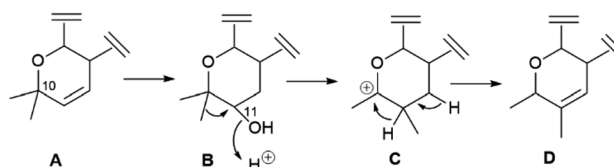
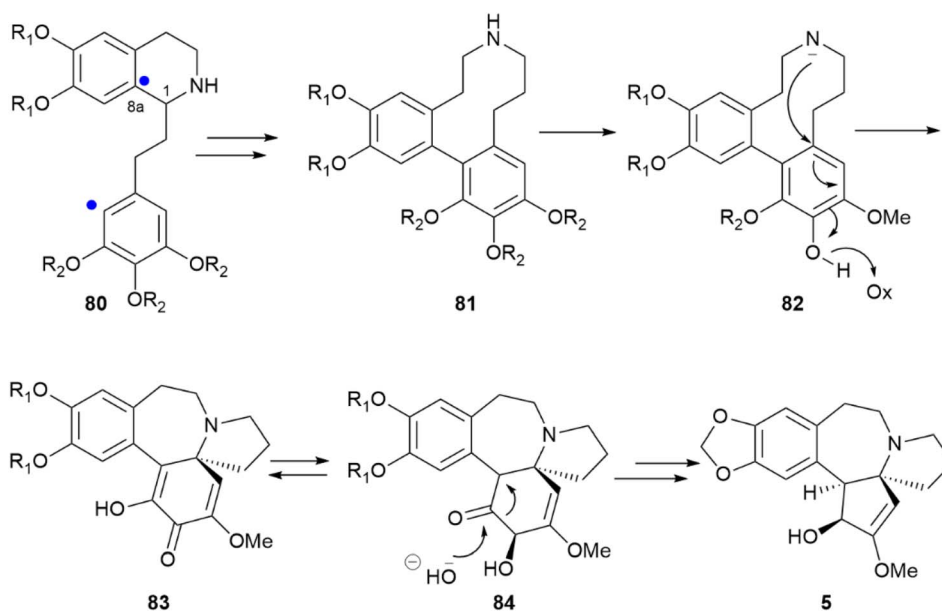


Fig. 16 Structure of calanolides A (85), calanolides B (86) and 4-propyldipetalolactone (87).



Scheme 19 Possible biogenetic derivation of the calanolide precursor 87 from a *gem*-dimethylated precursor (only the dihydropyran moiety is shown for clarity).

Calanolides are another remarkable example of substrate-controlled enantiospecific amplification of a scalemic stereocenter. These non-nucleoside reverse transcriptase inhibitors, exemplified by calanolides A and B (85 and 86, Fig. 16), have been isolated in a range of scalemic states as well as in more biologically active enantiopure form from various trees of the *Calophyllum* genus.<sup>118,119</sup> Calanolides are a veritable *apex* in the literature of anti-HIV drugs, not only for their non-nucleoside nature, but also for ability to alternatively bind two distinct sites of reverse transcriptase. In calanolide-producing plants,



Scheme 18 Biosynthesis of the alkaloid cephalotaxine (5) from a phenethylisoquinoline precursor (80).  $R_1 = \text{OH}$  or  $-\text{CH}_2-$ ;  $R_2 = \text{OH}$  or  $\text{OMe}$ . The sites of aryl coupling are indicated by a blue dot.



from an achiral *gem*-dimethyl substituted pyranocoumarin (simplified in Scheme 19 as A), a chiral compound is generated in scalemic form by hydration (Scheme 19B), Wagner-Meerwein rearrangement of one of the *gem*-methyl groups (Scheme 19C), and hydride migration from C-11 to C-10 (Scheme 19D). The resulting *vic*-dimethyl substituted derivative [4-propyl dipetalolactone (**87**)] is then hydrated regioselectively to scalemic calanolides. The configuration at C-10 of **87** controls the final oxidative elaboration of the chromene double bond by specific oxygenases, affording in scalemic form all possible relative configurations at the three stereocenters. The conversion of chromene **87** into scalemic calanolides is, apparently, under genetic control, since different *Calophyllum* species contain calanolides of different optical purity.<sup>120</sup>

**3.2.4 Oxidative modification of isoprenoid residues.** Epoxidation of isoprenoid residues is a general strategy to trigger intramolecular reactions ultimately leading to the formation of oxygen rings, most frequently furans and pyrans, as well as carbocycles, overall increasing scaffold diversity. In most cases the epoxidation is enantioselective, with exclusive formation of one enantiomer, but scalemic isoprenyloxides have also been reported, like epoxythymols, a class of aromatic monoterpenoids exemplified by areolal (**88**, Fig. 17) and isolated both as scalemates and enantiomerically pure compounds from various asteraceous plants.<sup>121</sup> Under acidic conditions, opening of the epoxide ring of epoxythymols could generate a stabilized benzyl cation en route to racemization. Since acidic conditions, even mild like gravity column chromatography on silica gel, are difficult to avoid during the isolation of natural products, it is unclear if the scalemic state of areolal and its analogues is due to erosion of enantiopurity or, alternatively, to the agency of enzymes with antipodal enantioselectivity and/or sloppy

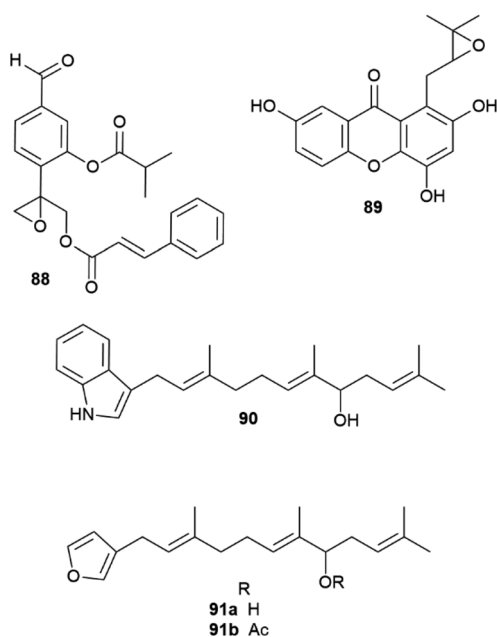


Fig. 17 Structure of epoxythymols (**88**), mangoxanthone B (**89**), 8-farnesylindole (**90**), 12-hydroxyambliofuran (**91a**) and its acetate (**91b**).

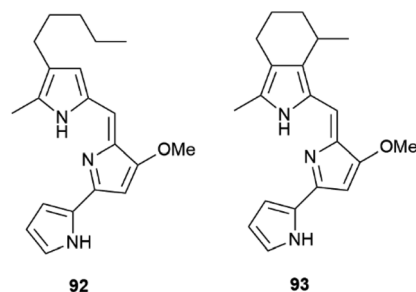
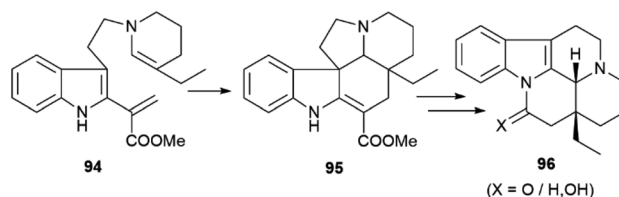


Fig. 18 Structure of prodigiosin (**92**) ancyloprodigiosin (**93**).

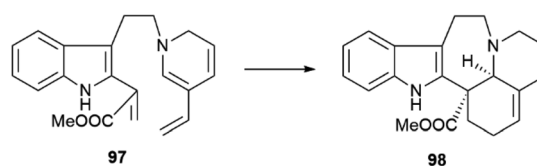


Scheme 20 Intramolecular cycloaddition in eburnane alkaloids from the genus *Kopsia*.

enantiodiscriminating activity.<sup>122</sup> On the other hand, the scalemic state of other isoprenyl oxides like mangoxanthone B (**89**)<sup>123</sup> seems of enzymatic origin, since its acid-induced racemization would involve anti-Markovnikov opening and formation of a non-stabilized secondary cation.

The allylic hydroxylation of isoprenoid moieties can also be associated to the generation of scalemates and racemates. Thus, 3-farnesylindole (**90**, Fig. 17) was isolated from *Anomianthus dulcis* in 33% ee in favour of the *R*-enantiomer,<sup>124</sup> and the marine furanoditerpene 12-hydroxyambliofuran (**91a**) and its acetate (**91b**) were obtained from a *Spongia* species as a ca. 3 : 1 mixture of enantiomers.<sup>125</sup>

**3.2.5 Functionalization of non-isoprenyl unactivated carbons.** The functionalization of unactivated carbons is carried out by iron-base monooxygenases and it is generally highly enantioselective, as observed in the metabolism of many drugs. On the other hand, scalemates can also be produced, either because of a poor enantiodifferentiation from the cytochrome active site, or because of the existence of enzymes with distinct enantioselectivity. The deep-red bacterial tripyrrole cycloprodigiosin (**93**, Fig. 18) is a remarkable example of C–H functionalization associated to production of a scalemate, and is derived from prodigiosin (**92**) by functionalization, in Friedel–Crafts sense, of the  $\omega$ -1 carbon of a *n*-pentyl chain.<sup>126</sup>



Scheme 21 Diels–Alder reaction in the formation of andranginine (**98**).



Many insect pheromones are also generated as scalemates by nonenantioselective hydroxylation of a non-activated carbon (see Section 6).<sup>127</sup>

**3.2.6 Cycloaddition reactions.** Natural products derived, at least formally, from a cycloaddition reaction are often racemic, unless a pre-existing stereocenter induces formation of a specific configuration. The isolation of optically pure or scalemic adducts is therefore indicative of enzymatic control. A remarkable case of enantiodivergent scalemicity was discovered in eburnane alkaloids from the genus *Kopsia*. The eburnane skeleton (**96**, Scheme 20) is biogenetically derived from an achiral secodine precursor (**94**) by intramolecular cycloaddition. This reverse electron demand Diels–Alder reaction generates an *Aspidosperma* cycloadduct (**95**) having three stereogenic centers, next further elaborated *en route* to eburnane derivatives.<sup>128</sup> Remarkably, the enantiomeric composition of many eburnane alkaloids in the same *Kopsia* species differed between collections done in Malaysia and in Borneo.<sup>128</sup>

A related regular demand Diels–Alder cycloaddition from the secodine precursor (**97**, Scheme 21) is involved in the formation of andranginine (**98**), a scalemic *Craspidospermum* alkaloid.<sup>129</sup>

## 4 Strategies to upgrade the optical purity of scalemic natural products

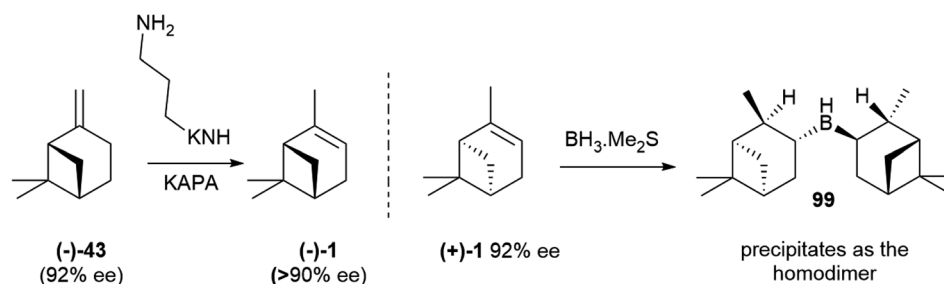
The occurrence of a chiral natural product as a scalemate or a racemate rather than in an enantiopure form has interesting implications, the most obvious being that both enantiomers are available by isolation. This is an important asset not only for bioactivity studies on structurally complex natural products, but also for all synthetic applications, both as chirons (chiral building blocks) and as chiral auxiliaries, catalysts and reagents in asymmetric synthesis. The flip side of the coin is, however, that the racemic and the scalemic states imply “optical impurity”, and resolution or an ee upgrade will be necessary. In terms of synthetic applications, the most important scalemic natural products is  $\alpha$ -pinene (**1**, Fig. 1). This monoterpene olefin and its derivatives have been extensively used as building blocks for the synthesis of natural and synthetic compounds and in asymmetric synthesis. For both uses, an upgrade of optical purity is necessary, since the ee of commercial  $\alpha$ -pinene **1** does not exceed 92% for the (+)-enantiomer ((+)-**1**) and 81% for the more expensive (–)-enantiomer ((–)-**1**). More optically pure (–)- $\alpha$ -pinene can be obtained by treatment of (–)- $\beta$ -pinene ((–)-**43**,

Scheme 22), available by isolation in up to 92% ee, with the potassium salt of 1,3-propandiamine (potassium 3-aminopropanamide, KAPA, Scheme 22 left). The superbases isomerizes the exocyclic double bond to the thermodynamically more stable endocyclic position, with deprotonation occurring selectively at the allylic methylene since the one at the allylic methine would generate an anti-Bredt allyl anion. In this way, also (–)-pinene becomes available in >90% optical purity.<sup>130</sup> Further upgrading of  $\alpha$ -pinenes capitalizes on the preparation of a homodimeric borane by reaction with diborane and equilibration with an excess of the starting scalemic  $\alpha$ -pinene (Scheme 22, right).<sup>130</sup> Due to steric hindrance, hydroboration stops at the dialkylborane (diisopinocampheylborane, Ipc<sub>2</sub>BH, **99**) stage. This, after evaporation of the solvent, is suspended in THF and equilibrated with an excess of  $\alpha$ -pinene. Statistic considerations favour the formation of the homodimeric borane, which precipitates from the reaction mixture. Enantiomerically upgraded  $\alpha$ -pinenes (**1** (>99% ee)) could then be obtained by decomposition of the borane. The resulting diisopinocampheylborane Ipc<sub>2</sub>BH **99** has multiple uses in asymmetric synthesis.<sup>131,132</sup>

## 5 Analytical applications of scalemic natural products

The determination of the enantiomeric excess of scalemic constituents provides an important asset for quality control, with interesting applications in the realm of essential oil authentication and food chemistry. Volatile scalemic monoterpenoids have proven useful to fight adulteration in the market of essential oils.<sup>133</sup>

Due to a high natural variability of composition, the definition of a reference profile for an essential oil requires the analysis of a large number of certified genuine samples, and is expressed, at least for those having an official monograph like the European Pharmacopoeia, into specific ranges of concentration, or of concentration ratios, for key markers.<sup>133</sup> Even so, the analytical landscape can be complicated by the presence of multiple botanical sources, by additional manipulation like rectification to remove sesquiterpenes or dilution with turpentine, as well as by intended or unintended exchange of raw material. In this scenario, the determination of the dominant enantiomer of a scalemic constituent can be a precious asset for authentication, as exemplified by the analysis of “pine oil”.



Scheme 22 Upgrading the optical purity of  $\alpha$ -pinenes (from ref. 130).



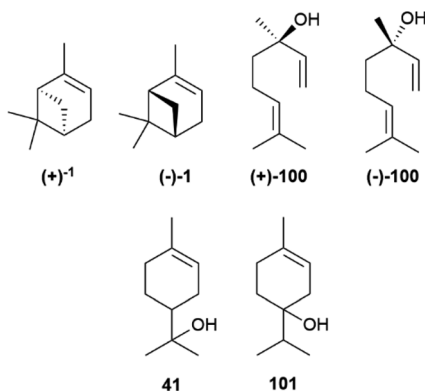


Fig. 19 Monoterpene markers of Scots pine, citrus, lime and tea tree essential oils.

Scalemic  $\alpha$ -pinene is the major constituents of pine oils of different botanical origin and commercial value.<sup>134</sup> In the essential oils from Scots pine (*Pinus sylvestris* L.), *P. cembra* L., and *P. sibirica* Du Tour, the (+) enantiomer (**1**, Fig. 19) prevails, while in those from *P. nigra* J. F. Arnold and *P. mugo* Turra (–)- $\alpha$ -pinene (**1**) dominates. The oil from *P. sylvestris* is the one of highest market value, but an analysis of several commercial samples labelled as *P. sylvestris* and complying with the European Pharmacopoeia criteria for this oil, actually showed a predominance of the (–) rather than the (+) enantiomer.<sup>134</sup> This, coupled with the overall profile of the oils, identified *P. nigra*, a major turpentine source, as the probable adulterant.<sup>134</sup>

A similar situation exists for “citrus oils”, where the determination of linalool enantiomeric ratio is useful to distinguish between bitter- and sweet orange oils: in the more valuable bitter orange oil, (–)-linalool ((–)-**100**, Fig. 19) is the most abundant enantiomer (60–89%), while in sweet orange (+)-linalool ((+)-**100**) dominates.<sup>135</sup> A lower optical purity for linalool and its acetate is diagnostic of adulteration for the oil of bergamot and lavender.<sup>133</sup> The determination of enantiomeric ratios is also useful to identify the preparation process of an oil, as well as the geographical origin of the starting biomass. A combination of the enantiomeric ratios of linalool and  $\alpha$ -terpineol (**41**, Fig. 19) can distinguish between lime oils prepared with different contact time of the peel and the pulp of the fruit, with an increased scalemicity trait being diagnostic of a longer contact time,<sup>135</sup> while the composition of scalemic terpinen-4-ol **101** can distinguish between tea tree [*Melaleuca alternifolia* (Maiden & Betche) Cheel] oils of Australian and Chinese origin.<sup>133,136</sup> In the more valuable Australian oil, the *S*-enantiomer of **101** prevails, with a *ca* 55 : 45 enantiomeric ratio, while in the cheaper Chinese oil the *R*-enantiomer is more abundant, with an *R/S* enantiomer ratio of *ca*. 58 : 42. The terpinen-4-ol enantiomeric ratio is now included in the ISO 4730 monograph of tea tree oil.<sup>137</sup>

Milk contains only traces of proteinogenic amino acids from the D-series, a profile not significantly affected by pasteurization or sterilization, and associated to the presence of lactic bacteria. During storage, however, bacterial enzymatic activity and/or bacterial cell lysis increase the concentration of

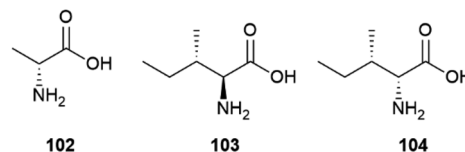


Fig. 20 Structure of proteinogenic amino acids used as biomarkers.

proteinogenic amino acids from the D-series, and especially D-alanine **102** (Fig. 20), a bacterial cell wall constituent.<sup>138</sup> The presence of D-amino acids increases steadily during cheese ripening, and in aged cheeses like Parmigiano Reggiano, the scalemicity of aspartic and glutamic acid can be used as a ripening marker.<sup>139</sup>

Interestingly, the scalemicity of certain proteinogenic amino acids can also be used to determine the age of fossilized human bones and teeth too old to be dated by <sup>14</sup>C-based isotopic analysis.<sup>140</sup> Thus, the content of D-aspartic acid in post-mortem dental enamel increases by *ca*. 0.1% every year due to spontaneous racemization and this, as well as the conversion of L-isoleucine (**103**) to D-alloisoleucine (**104**, Fig. 20) has also proved useful to age estimation up to one million year of fossilized human dental remains.<sup>141</sup>

## 6 The importance of being scalemic: when optical impurity is advantageous

The biological profile of enantiomeric natural products is rarely overlapping, although remarkable examples of lack of enantioselective activity are known, as exemplified by the nicotinic frog alkaloid epibatidine (**105**, Fig. 21).<sup>142</sup> In many cases, the activity of a scalemate can be approximated by a “weighed” combination of the one of its constituents, but significant deviations from this linear analysis have been reported with insects pheromones, where it is not uncommon that both enantiomers are recognized, but elicit distinct activity.<sup>127</sup> Chirality is a critical aspect of insect communication, but it is still a poorly known process involving both olfactory receptors and their associated odorant-binding proteins, which often show promiscuous binding toward enantiomers.<sup>143</sup> On the other hand, many insect pheromones are linear compounds whose structure show low conformational constraint to assist

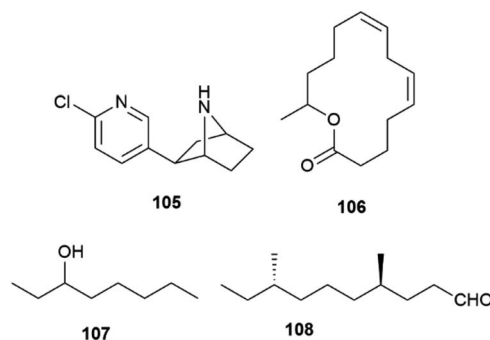


Fig. 21 Structure of some chiral pheromones.



recognition by a macromolecule.<sup>143</sup> Using enantiopure synthetic versions of chiral pheromones, it was surprisingly demonstrated that in some cases a well-defined scalemic version is necessary for optimal activity. Thus, the macrolide pheromone **106** of the grain beetle *Cryptolestes turcicus* showed activity only as a scalemic mixture, with an optimal ratio between the *R*- and *S*-enantiomers of 85 : 15, while both pure enantiomers were inactive.<sup>144,145</sup> In other cases, a scalemate simply outperformed its enantiomeric constituents as well as its corresponding racemic mixture. Studies on *Myrmica scabrinodis* demonstrated that the 9 : 1 scalemate of octan-3-ol **107** was more potent than the *R*-enantiomer, while the *S*-form was inactive.<sup>146</sup> Also interesting is the observation that the most potent stereochemical version of tribolure **108**, the aggregation pheromone of the red flour beetle (*Tribolium castaneum*), a worldwide pest of stored products, is a 4 : 1 mixture of the (4*R*,8*R*)- and (4*R*,8*S*)-diastereomers, and none of the single diastereo- and enantiomerically pure forms is found.<sup>147</sup> The combined activation of distinct receptors with different affinity for their enantiomeric (diastereomeric) ligands could underlie the need of a specific combination of isomers for bioactivity, but the precise details remain unknown. Insect olfactory receptors are ion channels, while the mammal olfactory receptors are GPCR, and their regulation is presumably distinct, while the ability of insect olfactory receptors to discriminate isotopomers is still highly debated for its implication on the theory of olfaction.<sup>148</sup>

## 7 Conclusions

The scalemic state of natural products seems to have been largely underestimated in terms of both inventory and biogenetic implications. It is generally associated, either directly or *via* directing protein, with enzymatic activity, and is common in specific classes of chiral compounds, like monoterpene hydrocarbons and biaryls. Also the intramolecular trapping of iminium ions can be associated with a non-negligible production of scalemates. However, additional enzymatic activity can lead to kinetic resolution *via* the enantioselective elaboration of only one enantiomer, as shown for nicotine in tobacco leaves. The enantiomer not recognized by downstream enzymes can be significantly accumulated, like *ent*-oxidosqualene (**109**, Fig. 22), not a substrate for oxidosqualene cyclases and a major constituent of jasmine absolute,<sup>71</sup> or, alternatively, can be diverted to other metabolic pathways, although few systematic studies exist in this area.

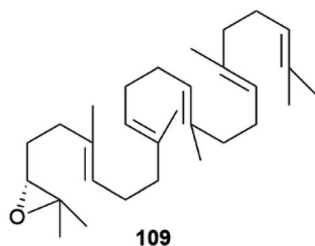


Fig. 22 3*R*-2,3-oxidosqualene (*ent*-squalene oxide), the enantiomeric triterpenoid from jasmine absolute.

Historically, optical activity was one of the first physicochemical properties associated to natural products and, indeed, chiral natural products are generally optically active, but not necessarily enantiopure. The production of racemic versions of specific chiral secondary metabolites is associated to the presence of non-enzymatic biogenetic steps or to spontaneous racemization, and can be viewed as a strategy of bioactivity expansion, since enantiomers rarely show an overlapping biological profile. A similar consideration applies to the production of scalemates, which, however, are generally the result of enzymatic activity, either direct or mediated by directing proteins, and therefore more “expensive” in genomic terms. This genomic profligacy could be viewed as a manoeuvre to increase the diversity of a natural products inventory and better adapted it to a specific environment, a view supported by the strong activity on insects of many terpenes and sesquiterpenes synthesized as scalemates (see Section 6). Compared to the production of racemic compounds, the production of scalemates is plastic and environmentally tunable, as shown by the spectacular gradient of  $\alpha$ -pinene configuration and scalemicity in the Amazon rainforest emission,<sup>149</sup> a chiral circadian show affected by altitude, temperature and herbivore activity, and for which we appreciate the *quid*, but do not understand the *quia*.

## 8 Author contributions

All authors equally contributed to the review, with the corresponding author coordinating their activity and conceptualizing the topic of this review.

## 9 Conflicts of interest

There are no conflicts to declare.

## 10 Acknowledgements

We would like to dedicate this article to the memory of Dr Daniele Ciceri, too prematurely taken from the affection of his family and from our friendship.

## 11 Notes and references

- 1 C. H. Hertzy, *J. Am. Chem. Soc.*, 1908, **30**, 863–867.
- 2 A. Findlay, *Nature*, 1937, **140**, 1937.
- 3 S. Scholtz, L. MacMorris, F. Krogmann and G. U. Auffarth, *J. Eye Study Treat.*, 2019, **1**, 51–58.
- 4 L. M. Bouthillette, V. Aniebok, D. A. Colosimo, D. Brumley and J. B. Macmillan, *Chem. Rev.*, 2022, **122**, 14815–14841.
- 5 R. J. Nyamwihura and I. V. Ogungbe, *RSC Adv.*, 2022, **12**, 11346–11375.
- 6 M. A. Schafroth, G. Mazzocanti, I. Reynoso-Moreno, R. Erni, F. Pollastro, D. Caprioglio, B. Botta, G. Allegrone, G. Grassi, A. Chicca, F. Gasparrini, J. Gertsch, E. M. Carreira and G. Appendino, *J. Nat. Prod.*, 2021, **84**, 2502–2510.
- 7 W. Huang and Y. X. Li, *Sci. Sin.*, 1980, **23**, 835.
- 8 G. Bredig and P. S. Fiske, *Biochem. Z.*, 1912, **46**, 7–23.



- 9 E. N. Jacobsen, I. Markó, W. S. Mungall, G. Schroder and K. B. Sharpless, *J. Am. Chem. Soc.*, 1988, **110**, 1968–1970.
- 10 J. M. Finefield, D. H. Sherman, M. Kreitman and R. M. Williams, *Angew. Chem., Int. Ed.*, 2012, **51**, 4802–4836.
- 11 A. Zask and G. Ellestad, *Chirality*, 2018, **30**, 157–164.
- 12 A. J. E. Novak and D. Trauner, *Trends Chem.*, 2020, **2**, 1052–1065.
- 13 A. Zask and G. A. Ellestad, *Chirality*, 2021, **33**, 915–930.
- 14 G. T. M. Bitchagno, V. A. Nchiozem-Ngnitedem, D. Melchert and S. A. Fobofou, *Nat. Rev. Chem.*, 2022, **6**, 806–822.
- 15 J.-H. Yu, Z.-P. Yu, R. J. Capon and H. Zhang, *Molecules*, 2022, **27**, 1279.
- 16 J. M. Batista, E. W. Blanch and V. Da Silva Bolzani, *Nat. Prod. Rep.*, 2015, **32**, 1280–1302.
- 17 J. Han, A. Wzorek, K. D. Klika and V. A. Soloshonok, *Molecules*, 2021, **26**, 2757.
- 18 B. Cai, A. M. Jack, R. S. Lewis, R. E. Dewey and L. P. Bush, *Phytochemistry*, 2013, **95**, 188–196.
- 19 S. T. Lee, K. Wildeboer, K. E. Panter, W. R. Kem, D. R. Gardner, R. J. Molyneux, C. W. T. Chang, F. Soti and J. A. Pfister, *Neurotoxicol. Teratol.*, 2006, **28**, 220–228.
- 20 A. K. Duell, P. J. Kerber, W. Luo and D. H. Peyton, *Chem. Res. Toxicol.*, 2021, **34**, 1718–1720.
- 21 J. Han, O. Kitagawa, A. Wzorek, K. D. Klika and V. A. Soloshonok, *Chem. Sci.*, 2018, **9**, 1718–1739.
- 22 S. Abás, C. Arróniz, E. Molins and C. Escolano, *Tetrahedron*, 2018, **74**, 867–871.
- 23 H. Doucet, E. Fernandez, T. P. Layzell and J. M. Brown, *Chem.–Eur. J.*, 1999, **5**, 1320–1330.
- 24 S. Tsuzuki, H. Orita, H. Ueki and V. A. Soloshonok, *J. Fluorine Chem.*, 2010, **131**, 461–466.
- 25 O. Wallach, *Justus Liebigs Ann. Chem.*, 1895, **286**, 119–143.
- 26 C. P. Brock, W. B. Schweizer and J. D. Dunitz, *J. Am. Chem. Soc.*, 1991, **113**, 9811–9820.
- 27 O. Ryu and K. B. Sharpless, *Org. Synth.*, 1998, **9**, 251.
- 28 Y. Mastai, A. Völkel and H. Cölfen, *J. Am. Chem. Soc.*, 2008, **130**, 2426–2427.
- 29 H. Lorenz, A. Perlberg, D. Sapoundjiev, M. P. Elsner and A. Seidel-Morgenstern, *Chem. Eng. Process.: Process Intensif.*, 2006, **45**, 863–873.
- 30 M. Masi, A. Cimmino, A. Boari, M. Chiara, G. Marcin, G. Pescitelli, A. Tuzi, M. Vurro and A. Evidente, *Tetrahedron*, 2017, **73**, 6644–6650.
- 31 W. -L. Tsai, K. Hermann, E. Hug, B. Rohde and A. S. Dreiding, *Helv. Chim. Acta*, 1985, **68**, 2238–2243.
- 32 P. Diter, S. Taudien, O. Samuel and H. B. Kagan, *J. Org. Chem.*, 1994, **59**, 370–373.
- 33 F. J. Muhtadi and M. M. A. Hassan, in *Analytical Profiles of Drug Substances*, ed. Florey K., 1990, pp. 477–551.
- 34 K. L. Kohnen-Johannsen and O. Kayser, *Molecules*, 2019, **24**, 796.
- 35 A. R. Cushny, *J. Pharmacol. Exp. Ther.*, 1920, **15**, 105–127.
- 36 *Scopolamine e atropine Polarim. test; Eur. Pharmacopoeia*, <https://pheur.edqm.eu/home>.
- 37 W. D. Dettbarn, E. Heilbronn, F. C. G. Hoskin and R. Kitz, *Neuropharmacology*, 1972, **11**, 727–732.
- 38 I. V. Alabugin, in *Stereoelectronic Effects: a Bridge Between Structure and Reactivity*, Wiley, 2016, pp. 8–36.
- 39 C. Tanret, *Hebd. Scéances Acad. Sci.*, 1878, **86**, 1270–1272.
- 40 R. Willstätter and E. Waser, *Ber. Dtsch. Chem. Ges.*, 1911, **44**, 3423–3445.
- 41 D. Sicker, K.-P. Zeller, H.-U. Siehl and S. Berger, in *Natural Products. Isolation, Structure Elucidation and Synthesis*, Wiley-VCH, 2020, Supporting Information to Chapter 1.
- 42 R. E. Gilman and L. Marion, *Bull. Soc. Chim. Fr.*, 1961, 1993–1995.
- 43 A. Kubin, F. Wierrani, U. Burner, G. Alth and W. Grunberger, *Curr. Pharm. Des.*, 2005, **11**, 233–253.
- 44 H. P. Bais, R. Vepachedu, C. B. Lawrence, F. R. Stermitz and J. M. Vivanco, *J. Biol. Chem.*, 2003, **278**, 32413–32422.
- 45 D. Skalkos, E. Tatsis, I. P. Gerothanassis and A. Troganis, *Tetrahedron*, 2002, **58**, 1925–4929.
- 46 R. Altmann, C. Etzlstorfer and H. Falk, *Monatsh. Chem.*, 1997, **128**, 785–793.
- 47 S. P. B. Vemulapalli, J. C. Fuentes-Monteverde, N. Karschin, T. Oji, C. Griesinger and K. Wolkenstein, *Mar. Drugs*, 2021, **19**, 445.
- 48 M. Iijima, R. Munakata, H. Takahashi, H. Kenmoku, R. Nakagawa, T. Kodama, Y. Asakawa, I. Abe, K. Yazaki, F. Kurosaki and F. Taura, *Plant Physiol.*, 2017, **174**, 2213–2230.
- 49 D. Caprioglio, D. Mattoteia, A. Minassi, F. Pollastro, A. Lopatriello, E. Muñoz, O. Tagliatela-Scafati and G. Appendino, *Org. Lett.*, 2019, **21**, 6122–6125.
- 50 Y. Kashiwada, K. Yamazaki, Y. Ikeshiro, T. Yamagishi, T. Fujioka, K. Mihashi, K. Mizuki, L. M. Cosentino, K. Fowke, S. L. Morris-Natschke and K. H. Lee, *Tetrahedron*, 2001, **57**, 1559–1563.
- 51 G. Mazzocanti, O. H. Ismail, I. D'Acquarica, C. Villani, C. Manzo, M. Wilcox, A. Cavazzini and F. Gasparrini, *Chem. Commun.*, 2017, **53**, 12262–12265.
- 52 F. Pollastro, D. Caprioglio, D. Del Prete, F. Rogati, A. Minassi, O. Tagliatela-Scafati, E. Munoz and G. Appendino, *Nat. Prod. Commun.*, 2018, **13**, 1189–1194.
- 53 H. Jeon, G. Kang, M. J. Kim, J. S. Shin, S. Han and H. Y. Lee, *Org. Lett.*, 2022, **24**, 2181–2185.
- 54 L. O. Hanuš, S. M. Meyer, E. Muñoz, O. Tagliatela-Scafati and G. Appendino, *Nat. Prod. Rep.*, 2016, **33**, 1357–1392.
- 55 G. Genchi, *Amino Acids*, 2017, **49**, 1521–1533.
- 56 T. Yoshimura and N. Esaki, *J. Biosci. Bioeng.*, 2003, **96**, 103–109.
- 57 A. Hashimoto, T. Nishikawa, T. Oka and K. Takahashi, *J. Neurochem.*, 1993, **60**, 783–786.
- 58 D. S. Dunlop, A. Neidle, D. McHale, D. M. Dunlop and A. Lajtha, *Biochem. Biophys. Res. Commun.*, 1986, **141**, 27–32.
- 59 A. Hashimoto, S. Kumashiro, T. Nishikawa, T. Oka, K. Takahashi, T. Mito, S. Takashima, N. Doi, Y. Mizutani, T. Yamazaki, T. Kaneko and E. Ootomo, *J. Neurochem.*, 1993, **61**, 348–351.
- 60 A. P. Kuzin, T. Sun, J. Jorczak-Baillass, V. L. Healy, C. T. Walsh and J. R. Knox, *Structure*, 2000, **8**, 463–470.
- 61 J. Gal, *Chirality*, 2012, **24**, 959–976.
- 62 L. Colli and A. Guarna, *Substantia*, 2018, **2**, 125–130.



- 63 G. C. Tron, A. Minassi, G. Sorba, M. Fausone and G. Appendino, *Beilstein J. Org. Chem.*, 2021, **17**, 1335–1351.
- 64 J. Gal, *Helv. Chim. Acta*, 2013, **96**, 1617–1657.
- 65 A. S. Tsarkova, *Front. Ecol. Evol.*, 2021, **9**, 667829.
- 66 Y. Oba, N. Yoshida, S. Kanie, M. Ojika and S. Inouye, *PLoS One*, 2013, **8**, e84023.
- 67 J. Maeda, D. Kato, M. Okuda, M. Takeo, S. Negoro, K. Arima, Y. Ito and K. Niwa, *Biochim. Biophys. Acta Gen. Subj.*, 2017, **1861**, 2112–2118.
- 68 S. Kanie, T. Nishikawa, M. Ojika and Y. Oba, *Sci. Rep.*, 2016, **6**, 24794.
- 69 R. Zhang, J. He, Z. Dong, G. Liu, Y. Yin, X. Zhang, Q. Li, Y. Ren, Y. Yang, W. Liu, X. Chen, W. Xia, K. Duan, F. Hao, Z. Lin, J. Yang, Z. Chang, R. Zhao, W. Wan, S. Lu, Y. Peng, S. Ge, W. Wang and X. Li, *Sci. Rep.*, 2020, **10**, 15882.
- 70 W. Liu, in *Handbook of Chiral Chemicals*, ed. D. J. Ager, 1999, pp. 83–102.
- 71 D. Joulain, *Flavour Fragr. J.*, 2021, **36**, 526–553.
- 72 J. F. Biellmann, *Chem. Rev.*, 2003, **103**, 2019–2033.
- 73 U. Bathe and A. Tissier, *Phytochemistry*, 2019, **161**, 149–162.
- 74 M. A. Phillips, M. R. Wildung, D. C. Williams, D. C. Hyatt and R. Croteau, *Arch. Biochem. Biophys.*, 2003, **411**, 267–276.
- 75 I. Prosser, I. G. Altug, A. L. Phillips, W. A. König, H. J. Bouwmeester and M. H. Beale, *Arch. Biochem. Biophys.*, 2004, **432**, 136–144.
- 76 S. Sarria, B. Wong, H. G. Martín, J. D. Keasling and P. Peralta-Yahya, *ACS Synth. Biol.*, 2014, **3**, 466–475.
- 77 J. Degenhardt, T. G. Köllner and J. Gershenzon, *Phytochemistry*, 2009, **70**, 1621–1637.
- 78 J. Bohlmann, C. L. Steele and R. Croteau, *J. Biol. Chem.*, 1997, **272**, 21784–21792.
- 79 S. Nix, *Ten most common trees in the United States*, <https://www.treehugger.com/ten-most-common-trees-united-states-3971258>.
- 80 C. O. Schmidt, H. J. Bouwmeester, S. Franke and W. A. König, *Chirality*, 1999, **11**, 353–362.
- 81 C. S. Chanotiya and A. Yadav, *Nat. Prod. Commun.*, 2008, **3**, 263–266.
- 82 S. T. Lee, D. R. Gardner, C. W. T. Chang, K. E. Panter and R. J. Molyneux, *Phytochem. Anal.*, 2008, **19**, 395–402.
- 83 A. W. Hofmann, *Ber. Dtsch. Chem. Ges.*, 1881, **14**, 705–713.
- 84 A. Ladenburg, *Ber. Dtsch. Chem. Ges.*, 1886, **19**, 439–441.
- 85 S. T. Lee, B. T. Green, K. D. Welch, G. T. Jordan, Q. Zhang, K. E. Panter, D. Hughes, C. W. T. Chang, J. A. Pfister and D. R. Gardner, *Chem. Res. Toxicol.*, 2008, **21**, 2061–2064.
- 86 L. M. Labay, A. Chan-Hosokawa, J. W. Homan, M. M. McMullin, F. X. Diamond, M. M. Annand, S. M. Marco and J. M. Hollenbach, *Forensic Sci. Int.*, 2022, **341**, 111500.
- 87 K. A. Yeung, P. R. Chai, B. L. Russell and T. B. Erickson, *J. Med. Toxicol.*, 2022, **18**, 321–333.
- 88 M. F. Roberts, *Phytochemistry*, 1975, **14**, 2393–2397.
- 89 G. Peddinti, H. Hotti, T. H. Teeri and H. Rischer, *Sci. Rep.*, 2022, **12**, 17562.
- 90 N. V. Mody, R. Henson, P. A. Hedin, U. Kokpol and D. H. Miles, *Experientia*, 1976, **32**, 829–830.
- 91 D. W. Armstrong, X. Wang, J. T. Lee and Y. S. Liu, *Chirality*, 1999, **11**, 82–84.
- 92 M. Kajikawa, N. Sierro, H. Kawaguchi, N. Bakaher, N. V. Ivanov, T. Hashimoto and T. Shoji, *Plant Physiol.*, 2017, **174**, 999–1011.
- 93 A. J. Deng, H. J. Zhang, Q. Li, Z. H. Li, Z. H. Zhang, L. Q. Wu, L. Li and H. L. Qin, *Phytochemistry*, 2017, **144**, 159–170.
- 94 S. Suzuki, *Wood Res.*, 2002, **89**, 52–60.
- 95 T. Umezawa, *Phytochem. Rev.*, 2003, **2**, 371–390.
- 96 L. Jin, Z. Song, F. Cai, L. Ruan and R. Jiang, *Molecules*, 2023, **28**, 302.
- 97 C. T. Walsh and B. S. Moore, *Angew. Chem., Int. Ed.*, 2019, **58**, 6846–6879.
- 98 L. B. Davin, H. Bin Wang, A. L. Crowell, D. L. Bedgar, D. M. Martin, S. Sarkanen and N. G. Lewis, *Science*, 1997, **275**, 362–366.
- 99 L. B. Davin and N. G. Lewis, *Plant Physiol.*, 2000, **123**, 453–461.
- 100 K. W. Kim, C. A. Smith, M. D. Daily, J. R. Cort, L. B. Davin and N. G. Lewis, *J. Biol. Chem.*, 2015, **290**, 1308–1318.
- 101 B. Pickel, M. A. Constantin, J. Pfannstiel, J. Conrad, U. Beifuss and A. Schaller, *Angew. Chem., Int. Ed.*, 2010, **49**, 202–204.
- 102 R. Gasper, I. Effenberger, P. Kolesinski, B. Terlecka, E. Hofmann and A. Schaller, *Plant Physiol.*, 2016, **172**, 2165–2175.
- 103 S. Suzuki, T. Umezawa and M. Shimada, *Biosci., Biotechnol., Biochem.*, 2002, **66**, 1262–1269.
- 104 S. C. Halls, L. B. Davin, D. M. Kramer and N. G. Lewis, *Biochemistry*, 2004, **43**, 2587–2595.
- 105 A. T. Dinkova-Kostova, D. R. Gang, L. B. Davin, D. L. Bedgar, A. Chu and N. G. Lewis, *J. Biol. Chem.*, 1996, **271**, 29473–29482.
- 106 T. Okunishi, T. Umezawa and M. Shimada, *J. Wood Sci.*, 2000, **46**, 234–242.
- 107 D. T. Tshitenge, D. Feineis, S. Awale and G. Bringmann, *J. Nat. Prod.*, 2017, **80**, 1604–1614.
- 108 N. Ikezawa, K. Iwasa and F. Sato, *J. Biol. Chem.*, 2008, **283**, 8810–8821.
- 109 C. Li, C. J. Li, J. Ma, J. W. Huang, X. Y. Wang, X. L. Wang, F. Ye and D. M. Zhang, *Bioorg. Chem.*, 2019, **88**, 102948.
- 110 Z. Yang, B. Su, Y. Wang, H. Liao, Z. Chen and D. Liang, *J. Nat. Prod.*, 2020, **83**, 985–995.
- 111 Y. Kinoshita, Y. Yamamoto, I. Yoshimura, T. Kurokawa and S. Huneck, *J. Hattori Bot. Lab.*, 1997, **83**, 173–178.
- 112 S. Chitturi and G. C. Farrell, *J. Gastroenterol. Hepatol.*, 2008, **23**, 366–373.
- 113 A. Galanty, P. Paško and I. Podolak, *Phytochem. Rev.*, 2019, **18**, 527–548.
- 114 Y. Liu, L. Wang, L. Zhao and Y. Zhang, *Nat. Prod. Rep.*, 2022, **39**, 1282–1304.
- 115 I. Effenberger, B. Zhang, L. Li, Q. Wang, Y. Liu, I. Klaiber, J. Pfannstiel, Q. Wang and A. Schaller, *Angew. Chem., Int. Ed.*, 2015, **54**, 14660–14663.
- 116 W. Fang, S. Ji, N. Jiang, W. Wang, G. Y. Zhao, S. Zhang, H. M. Ge, Q. Xu, A. H. Zhang, Y. L. Zhang, Y. C. Song, J. Zhang and R. X. Tan, *Nat. Commun.*, 2012, **3**, 1039.





- 117 P. Allegrini and G. Appendino, *Manuscr. Prep.*
- 118 L. Nahar, A. Das Talukdar, D. Nath, S. Nath, A. Mehan, F. M. D. Ismail and S. D. Sarker, *Molecules*, 2020, **25**, 4983.
- 119 J. H. Cardellina, H. R. Bokesch, T. C. McKee and M. R. Boyd, *Bioorganic Med. Chem. Lett.*, 1995, **5**, 1011–1014.
- 120 M. Mariner, B. McMahon and R. Boyd, *J. Pharmacol. Exp. Ther.*, 1996, **279**, 652–661.
- 121 M. Arreaga-Gonz, A. J. Oliveros-Ortiz, E. Rosa, G. Rodr, J. M. Torres-Valencia, C. M. Cerda-Garc, P. Joseph-Nathan and A. G. Mario, *J. Nat. Prod.*, 2021, **84**, 707–712.
- 122 H. M. Arreaga-González, G. Rodríguez-García, R. E. Del Río, J. A. Ferreira-Sereno, H. A. García-Gutiérrez, C. M. Cerda-García-Rojas, P. Joseph-Nathan and M. A. Gómez-Hurtado, *J. Nat. Prod.*, 2019, **82**, 3394–3400.
- 123 L. Yang, D. Zhang, J. B. Lia, X. Zhang, N. Zhou, W. Y. Zhang and H. Lu, *J. Asian Nat. Prod. Res.*, 2022, **24**, 624–633.
- 124 T. Promchai, T. Thaima, R. Rattanajak, S. Kamchonwongpaisan, S. G. Pyne and T. Limtharakul, *Nat. Prod. Res.*, 2021, **35**, 2476–2481.
- 125 P. A. Searle and F. Molinzi, *Tetrahedron*, 1994, **50**, 9893–9908.
- 126 R. E. Johnson, T. De Rond, V. N. G. Lindsay, J. D. Keasling and R. Sarpong, *Org. Lett.*, 2015, **17**, 3474–3477.
- 127 K. Mori, *Bioorg. Med. Chem.*, 2007, **15**, 7505–7523.
- 128 K. W. Chong, J. S. Y. Yeap, S. H. Lim, J. F. F. Weber, Y. Y. Low and T. S. Kam, *J. Nat. Prod.*, 2017, **80**, 3014–3024.
- 129 C. Kan-Fan, G. Massiot, A. Ahond, B. C. Das, H. P. Husson, P. Potier, A. I. Scott and C. C. Wei, *J. Chem. Soc., Chem. Commun.*, 1974, **5**, 164–165.
- 130 H. C. Brown and P. K. Jadhav, *J. Am. Chem. Soc.*, 1983, **105**, 2092–2093.
- 131 H. C. Brown and P. Veeraraghavan Ramachandran, *J. Organomet. Chem.*, 1995, **500**, 1–19.
- 132 I. Paterson, J. M. Goodman, M. Anne Lister, R. C. Schumann, C. K. McClure and R. D. Norcross, *Tetrahedron*, 1990, **46**, 4663–4684.
- 133 F. Capetti, A. Marengo, C. Cagliero, E. Liberto, C. Bicchi, P. Rubiolo and B. Sgorbini, *Molecules*, 2021, 5610.
- 134 M. Allenspach, C. Valder, D. Flamm and C. Steuer, *Sci. Rep.*, 2021, **11**, 16923.
- 135 I. Bonaccorsi, D. Sciarrone, A. Cotroneo, L. Mondello, P. Dugo and G. Dugo, *Rev. Bras. Farmacogn.*, 2011, **21**, 841–849.
- 136 N. W. Davies, T. Larkman, P. J. Marriott and I. A. Khan, *J. Agric. Food Chem.*, 2016, **64**, 4817–4819.
- 137 *Essential Oil of Melaleuca, Terpinen-4-ol Type (Tea Tree Oil)*, <http://www.iso.org/>.
- 138 I. Gandolfi, G. Palla, L. Delprato, F. D. E. Nisco and R. Marchelli, *J. Food Sci.*, 1992, **57**, 377–379.
- 139 F. Bellesia, A. Pinetti, L. Simon-sarkadi, C. Zucchi, J. Csapó, B. Weimer, L. Caglioti and G. Pályi, in *Advances in Asymmetric Autocatalysis and Related Topics*, 2017, pp. 357–367.
- 140 P. M. Helfman and J. L. Bada, *Nature*, 1976, **262**, 279–281.
- 141 G. Rainer, *Am. J. Phys. Anthropol.*, 2006, **48**, 2–48.
- 142 M. I. Damaj, K. R. Creasy, A. D. Grove, J. A. Rosecrans and B. R. Martin, *Brain Res.*, 1994, **664**, 34–40.
- 143 C. Sims, M. A. Birkett and D. M. Withall, *Insects*, 2022, **13**, 368.
- 144 A. C. Oehlschlager, G. G. S. King, H. D. Pierce, A. M. Pierce, K. N. Slessor, J. G. Millar and J. H. Borden, *J. Chem. Ecol.*, 1987, **13**, 1543–1554.
- 145 J. G. Millar, H. D. Pierce, A. M. Pierce, A. C. Oehlschlager and J. H. Borden, *J. Chem. Ecol.*, 1985, **11**, 1071–1081.
- 146 M. C. Cammaerts and K. Mori, *Physiol. Entomol.*, 1987, **12**, 381–385.
- 147 T. Suzuki, J. Kozaki, R. Sugawara and K. Mori, *Chem. Pharm. Bull.*, 1984, **19**, 15–20.
- 148 M. Paoli, A. Anesi, R. Antolini, G. Guella, G. Vallortigara and A. Haase, *Sci. Rep.*, 2016, **6**, 21893.
- 149 N. Zanoni, D. Leppla, P. I. Lembo Silveira de Assis, T. Hoffmann, M. Sá, A. Araújo and J. Williams, *Commun. Earth Environ.*, 2020, **1**, 1–11.

